Journal of Non-Crystalline Solids 461 (2017) 47–60

Contents lists available at ScienceDirect

Journal of Non-Crystalline Solids

journal homepage: www.elsevier.com/locate/jnoncrysol

Thermodynamic assessment of the phase equilibria and prediction of glass-forming ability of the Al–Cu–Zr system

Chenyang Zhou, Cuiping Guo *, Changrong Li, Zhenmin Du *

Department of Materials Science and Engineering, University of Science and Technology Beijing, Beijing 100083, PR China

ARTICLE INFO

Article history:
Received 6 July 2016
Received in revised form 26 September 2016
Accepted 27 September 2016
Available online 3 February 2017

Keywords:
Al–Cu–Zr system
CALPHAD method
Phase equilibria
Thermodynamic properties
Glass-forming ability

ABSTRACT

The thermodynamic description of the Al–Cu–Zr system was performed using the CALPHAD method. The solution phases liquid, fcc, bcc and hcp were described using a substitutional solution model. The compounds in the Al–Zr and Cu–Zr systems and the ternary compounds τ_3, τ_5, τ_7 and τ_8 were treated as a line compound in the Al–Cu–Zr system. The ternary compounds τ_1, τ_2, τ_4, τ_6, τ_9 and τ_{11} were described as a stoichiometric compound. The enthalpies of mixing of the liquid phase at different temperatures and compositions, two invariant reactions, and five isothermal sections at 773, 873, 1073, 1273 and 1373 K were taken into account in the present optimization work. A set of self-consistent and reliable thermodynamic parameters of the Al–Cu–Zr system was obtained. By searching the local minimum of the driving force for crystalline phases under the supercooled liquids, the thermodynamic parameters obtained in this assessment were later used for predicting composition dependencies of high glass-forming ability in the Al–Cu–Zr system. The predicted alloy compositions of high glass-forming ability are in satisfactory agreement with the available experimental data.

1. Introduction

Bulk metallic glasses (BMGs) with amorphous structure have aroused considerable interest because of their superior properties such as high strength, large elastic limit, good corrosion resistance, etc. [1]. It is well documented that Al–Cu–Zr alloys possess a high glass-forming ability (GFA) [2–4]. Recently, much attention has been paid to a series of Ni-free Al–Cu–Zr based BMGs. By alloying other elements Ag [5,6], Fe [7–9], Ti [10,11], Y [12–14], Nb and Pd [15–17] etc., the alloys with better mechanical properties, corrosion resistance and biocompatibility have been obtained. Therefore, Ni-free Al–Cu–Zr based BMGs are selected to be a perfect candidate for biomedical materials.

It is believed that GFA is a key factor in alloy design of BMGs. There have been several approaches to predict GFA. In the early stage, Greer [18] proposed a confusion principle indicating that the large number of elements leads to high GFA. Then, Inoue [1] summarized three well-known empirical rules, which are multicomponent systems, atomic size mismatch and negative heat of mixing, and also suggested that the alloy compositions with high GFA should be near eutectic points. Besides, several experimental rules have been developed to assess GFA on the basis of the results of the thermal analyses. Examples are given by $T_{rg} = T_g/T_m$ [19], $\Delta T_x = T_x - T_g$ [20], $\gamma = T_x/(T_g + T_m)$ [21] and $\delta = T_x/(T_m - T_g)$ [22]., where the essential data including the glass transition temperature (T_g), the melting temperature (T_m) and the crystallization temperature (T_x) can be acquired by experimental measurements.

In addition, many attempts have been used to predict the GFA on the basis of the CALPHAD method. Bormann [23] considered the contribution of the excess specific heat of the liquid phase in order to distinguish between the liquid phase and the amorphous one. Ågren et al. [24] proposed a two-state model, where the glass forming process is related to the gradual loss of translational energy. Shao et al. [25] treated the glass transition as the second-order phase transformation, and applied the same format with the magnetic transition to describe the Gibbs energy of the liquid-amorphous phase and to produce all useful indictors including T_g, T_m, and T_x. But these approaches still require many experimental data and are difficult to be extended to multicomponent system. In the present work, the approach proposed by Boettinger [26] to predict the high GFA with the local minimum of the driving force for crystalline phases under the supercooled liquids is adopted, which has been successfully applied to the following systems, such as Cu–Ti–Zr [27], Mg–Cu–Y [28], Ca–Mg–Zn [29] and La–Mg–Ni [30] ternary systems, Cu–Hf, Cu–Zr, Ni–Zr, Nb–Ni, Nb–Ni, Ti–Ni and Pd–Si [31] binary systems, etc.

To serve for high GFA prediction and further alloy design, the self-consistent and reliable thermodynamic parameters of the Al–Cu–Zr system are necessary. The CALPHAD method is a useful tool to acquire these parameters in the multicomponent systems. Therefore, the purpose of the present work is to obtain a set of self-consistent and reliable thermodynamic parameters using CALPHAD method and then adopt these parameters to predicting the alloy compositions of high GFA by

* Corresponding authors.
E-mail addresses: cpguo2003@sina.com (C. Guo), duzm@ustb.edu.cn (Z. Du).

http://dx.doi.org/10.1016/j.jnoncrysol.2016.09.031
0022-3093/

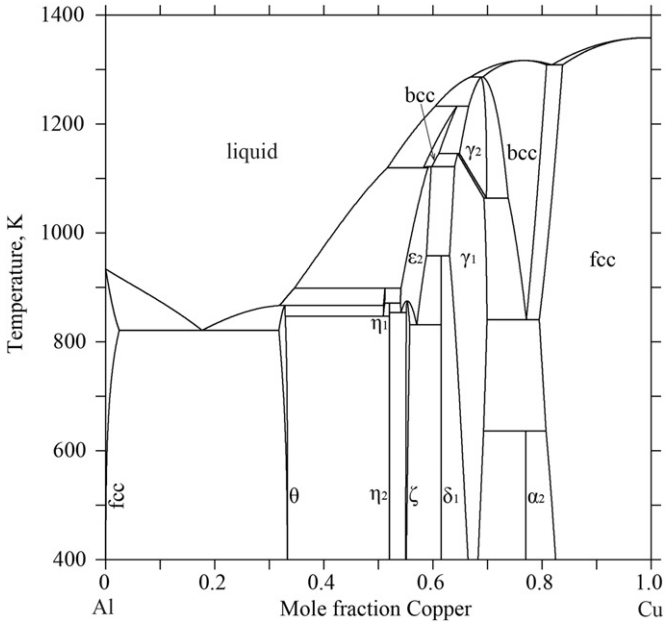

Fig. 1. Calculated Al–Cu phase diagram using the thermodynamic parameters from Liang and Schmid-Fetzer [36].

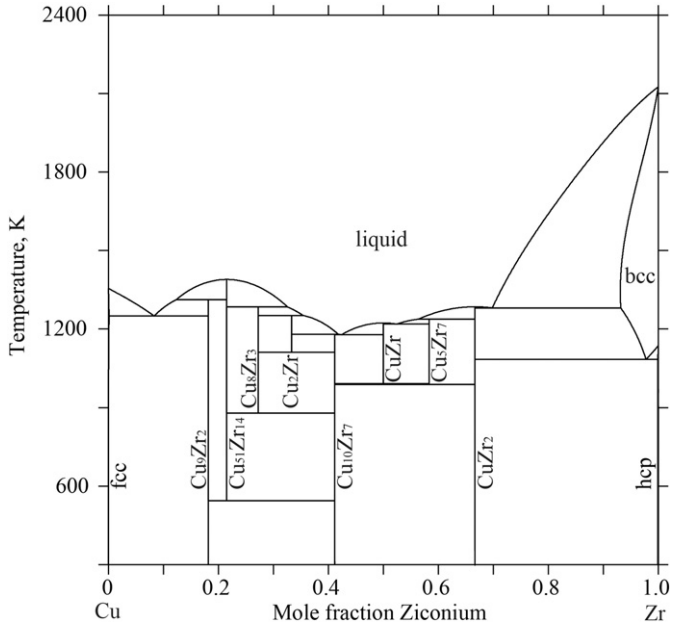

Fig. 3. Calculated Cu–Zr phase diagram using the thermodynamic parameters from Gierlotka et al. [57].

searching the local minimum of the driving force for crystalline phases under the supercooled liquids in the Al–Cu–Zr system.

2. Information on binary systems

To assess the Al–Cu–Zr ternary system using the CALPHAD method, the thermodynamic description of each binary system is necessary.

2.1. Al–Cu system

It is the thermochemical data of the Al–Cu system optimized by Saunders [32] that have been widely accepted in the multicomponent system. Based on the established description [32], Liang and Chang [33] described phase γ_1 as the sublattice model to match the solid solubilities of the Al–Cu–Zn system. Later, Miettinen [34] used the same model as [33] and revised partial thermodynamic parameters, but it was improper that their work only considered the Cu-rich part and no parameters in the Al-rich corner were provided. To improve the phase field of the phase γ_1 at temperatures lower than 600 K and temperature dependencies of the liquid phase, the thermodynamic

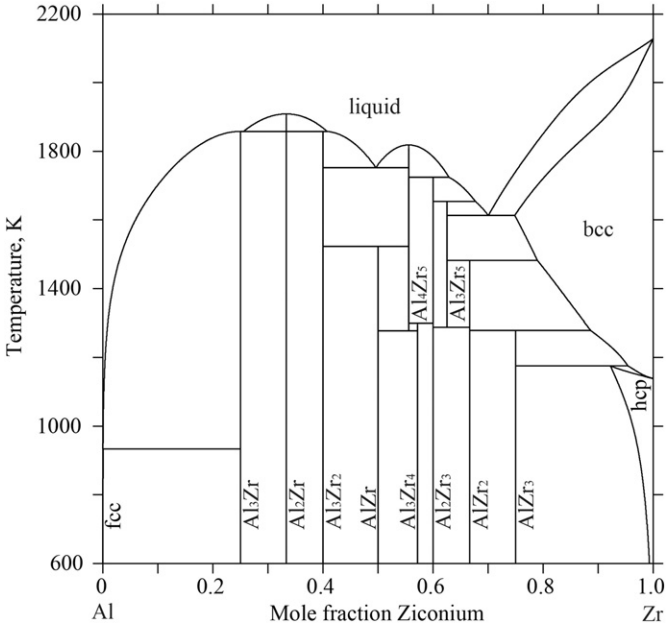

Fig. 2. Calculated Al–Zr phase diagram using the thermodynamic parameters from Fischer and Colinet [49].

Table 1
Crystallographic description and thermodynamic model of the binary compounds in the Al–Zr and Cu–Zr system and ternary compounds in the Al–Cu–Zr system.

Phase	Pearson symbol	Prototype	Thermodynamic model
Al_3Zr	*tI*16	Al_3Zr	$(Al,Cu)_3Zr$
Al_2Zr	*hP*12	$MgZn_2$	$(Al,Cu)_2Zr$
Al_3Zr_2	*oF*40	Al_3Zr_2	$(Al,Cu)_3Zr_2$
AlZr	*oC*8	CrB	(Al,Cu)Zr
Al_4Zr_5	*hP*18	Ga_4Ti_5	$(Al,Cu)_4Zr_5$
Al_3Zr_4	*hP*7	Al_3Zr_4	$(Al,Cu)_3Zr_4$
Al_2Zr_3	*tP*20	Al_2Zr_3	$(Al,Cu)_2Zr_3$
Al_3Zr_5	*tI*32	Si_3W_5	$(Al,Cu)_3Zr_5$
$AlZr_2$	*hP*6	Ni_2In	$(Al,Cu)Zr_2$
$AlZr_3$	*cP*4	Cu_3Au	$(Al,Cu)Zr_3$
Cu_9Zr_2	*cF*24	$AuBe_5$	$Cu_9(Al,Zr)_2$
$Cu_{51}Zr_{14}$	*hP*68	$Ag_{51}Gd_{14}$	$(Al,Cu)_{51}Zr_{14}$
Cu_8Zr_3	*oP*44	Cu_8Hf_3	$(Al,Cu)_8Zr_3$
Cu_2Zr	–	–	$(Al,Cu)_2Zr$
$Cu_{10}Zr_7$	*oC*68	$Ni_{10}Zr_7$	$(Al,Cu)_{10}Zr_7$
CuZr	*cP*2	CsCl	(Al,Cu)Zr
Cu_5Zr_7	–	–	$(Al,Cu)_5Zr_7$
$CuZr_2$	*tI*6	$MoSi_2$	$(Al,Cu)Zr_2$
τ_1	–	–	$Al_{14}Cu_{71}Zr_{15}$
τ_2	–	–	$Al_3Cu_6Zr_{16}$
τ_3	–	–	(Al,Cu)Zr
τ_4	*oF*16	$MnCu_2Al$	$AlCu_2Zr$
τ_5	*cF*24	$MgCu_2$	$(Al,Cu)_2Zr$
τ_6	–	–	Al_3Cu_4Zr
τ_7	*tI*26	$Mn_{12}Th$	$(Al,Cu)_{12}Zr$
τ_8	*cP*4	Cu_3Au	$(Al,Cu)_3Zr$
τ_9'[a]	–	–	–
τ_9	–	–	$Al_{68}Cu_{15}Zr_{17}$
τ_{10}[b]	*cF*116	$Mg_6Cu_{16}Si_7$	–
τ_{11}	–	–	$Al_{13}Cu_{79}Zr_8$

[a] It was not measured to exist by Soares and Castro [64].
[b] It was not measured to exist by Kalmykov et al. [70].

Table 2
Optimized thermodynamic parameters of the Al–Cu–Zr system[a].

Phase	Thermodynamic parameters	Reference
liquid: $(Al,Cu,Zr)_1$	${}^0L^{liq.}_{Al,Cu} = -67094.0+8.5550T$	[36]
	${}^1L^{liq.}_{Al,Cu} = +32148.0-7.1180T$	[36]
	${}^2L^{liq.}_{Al,Cu} = +5915.0-5.8890T$	[36]
	${}^3L^{liq.}_{Al,Cu} = -7290.0+5.5000T$	[36]
	${}^0L^{liq.}_{Al,Zr} = -184478.0+50.0330T$	[49]
	${}^1L^{liq.}_{Al,Zr} = -20276.5+7.3515T$	[49]
	${}^2L^{liq.}_{Al,Zr} = +48183.91-10.6230T$	[49]
	${}^0L^{liq.}_{Cu,Zr} = -140638.6+444.1606T -51.3121T\times \ln(T)$	[57]
	${}^1L^{liq.}_{Cu,Zr} = -22066.2+84.9923T -9.6125T\times \ln(T)$	[57]
	${}^2L^{liq.}_{Cu,Zr} = +56633.154-307.3817T +36.8512T\times \ln(T)$	[57]
	${}^3L^{liq.}_{Cu,Zr} = -22368.7+119.5438T -13.6488T\times \ln(T)$	[57]
	${}^0L^{liq.}_{Al,Cu,Zr} = -417439.6+100.2335T$	This work
	${}^1L^{liq.}_{Al,Cu,Zr} = +150013.2$	This work
fcc: $(Al,Cu,Zr)_1$	${}^0L^{fcc}_{Al,Cu} = -53520.0+2.0000T$	[36]
	${}^1L^{fcc}_{Al,Cu} = +39005.0-2.3680T$	[36]
	${}^2L^{fcc}_{Al,Cu} = +1210.0$	[36]
	${}^0L^{fcc}_{Al,Zr} = -140764.2+24.1562T$	[49]
	${}^0L^{fcc}_{Cu,Zr} = +8254.8$	[57]
bcc: $(Al,Cu,Zr)_1$	${}^0L^{bcc}_{Al,Cu} = -73537.0+3.9800T$	[36]
	${}^1L^{bcc}_{Al,Cu} = +51696.0-12.0000T$	[36]
	${}^0L^{bcc}_{Al,Zr} = -151558.7+26.0905T$	[49]
	${}^1L^{bcc}_{Al,Zr} = -32447.9$	[49]
	${}^2L^{bcc}_{Al,Zr} = +20000.0$	[49]
	${}^0L^{bcc}_{Cu,Zr} = +357.0-5.5499T$	[57]
	${}^0L^{bcc}_{Al,Cu,Zr} = +119787.7$	This work
	${}^1L^{bcc}_{Al,Cu,Zr} = +699876.7$	This work
	${}^2L^{bcc}_{Al,Cu,Zr} = -149956.6$	This work
hcp: $(Al,Cu,Zr)_1$	${}^0L^{hcp}_{Al,Zr} = -153421.2+40.4493T$	[49]
	${}^1L^{hcp}_{Al,Zr} = +12154.7$	[49]
	${}^2L^{hcp}_{Al,Zr} = +50000.0$	[49]
	${}^0L^{hcp}_{Cu,Zr} = -52576.6+70.9696T$	[57]
θ: $(Al)_2(Al,Cu)$	$G^{\theta}_{Al:Al} = 3GALBCC$	[36]
	$G^{\theta}_{Al:Cu} = 2GHSER_{Al}+GHSER_{Cu}-48361.0+8.0000T$	[36]
	${}^0L^{\theta}_{Al:Al,Cu} = +2211.0$	[36]
η_1: $(Al,Cu)(Cu)$	$G^{\eta_1}_{Al:Cu} = GHSER_{Al}+GHSER_{Cu}-39431.0+1.9000T$	[36]
	$G^{\eta_1}_{Cu:Cu} = 2GHSER_{Cu}+4770.0+9.0000T$	[36]
	${}^1L^{\eta_1}_{Al,Cu:Cu} = +43168.0-18.5000T$	[36]
η_2: $Al_{0.48}Cu_{0.52}$	$G^{\eta_2}_{Al:Cu} = 0.48GHSER_{Al}+0.52GHSER_{Cu}-20987.0+1.6200T$	[36]
ε_2: $(Al,Cu)(Cu)$	$G^{\varepsilon_2}_{Al:Cu} = GHSER_{Al}+GHSER_{Cu}-40326.0+4.1000T$	[36]
	$G^{\varepsilon_2}_{Cu:Cu} = 2GHSER_{Cu}+14850.0+30.1000T$	[36]
	${}^0L^{\varepsilon_2}_{Al,Cu:Cu} = -56870.0-55.0000T$	[36]
ζ: $(Al,Cu)_9(Cu)_{11}$	$G^{\zeta}_{Al:Cu} = 9GHSER_{Al}+11GHSER_{Cu}-424720.0+20.0000T$	[36]
	$G^{\zeta}_{Cu:Cu} = 20GCUBCC$	[36]
	${}^1L^{\zeta}_{Al,Cu:Cu} = -413300.0+100.0000T$	[36]
δ_1: Al_5Cu_8	$G^{\delta_1}_{Al:Cu} = 5GHSER_{Al}+8GHSER_{Cu}-278450.0+5.2000T$	[36]
γ_1: $(Cu)_4(Cu)_6(Al,Cu)_{16}$	$G^{\gamma_1}_{Cu:Cu:Al} = 16GHSER_{Al}+10GHSER_{Cu}-94322.4+389.5080T$	[36]
	$G^{\gamma_1}_{Cu:Cu:Cu} = 26GHSER_{Cu}+2600$	[36]
	${}^0L^{\gamma_1}_{Cu:Cu:Al,Cu} = -1613680.0-708.0000T$	[36]
	${}^1L^{\gamma_1}_{Cu:Cu:Al,Cu} = -1585780.0-100.0000T$	[36]
γ_2: $(Cu)_4(Cu)_6(Al,Cu)_{16}$	$G^{\gamma_2}_{Cu:Cu:Al} = 16GHSER_{Al}+10GHSER_{Cu}-94322.4+389.5080T$	[36]
	$G^{\gamma_2}_{Cu:Cu:Cu} = 26GHSER_{Cu}+2600$	[36]
	${}^0L^{\gamma_2}_{Cu:Cu:Al,Cu} = -1451526.6-859.6280T$	[36]
	${}^1L^{\gamma_2}_{Cu:Cu:Al,Cu} = -1516652.4-92.0000T$	[36]
α_2: $Al_{0.23}Cu_{0.77}$	$G^{\alpha_2}_{Al:Cu} = 0.23GHSER_{Al}+0.77GHSER_{Cu}-13904.9-3.0000T$	[36]
$Al_2Zr(\tau_5)$: $(Al,Cu)_2Zr$	$G^{Al_2Zr}_{Al:Zr} = 2GHSER_{Al}+GHSER_{Zr}-150858.0-78.7589T+13.2510T\ln T$	[49]
	$G^{Al_2Zr}_{Cu:Zr} = G^{Cu_2Zr}_{Cu:Zr}+15000.0$	This work
	${}^0L^{Al_2Zr}_{Al,Cu:Zr} = -257301.0+100.1201T$	This work
	${}^1L^{Al_2Zr}_{Al,Cu:Zr} = -19000.0$	This work
Al_3Zr_2: $(Al,Cu)_3Zr_2$	$G^{Al_3Zr_2}_{Al:Zr} = 3GHSER_{Al}+2GHSER_{Zr}-243045.0-134.8002T+21.6450T\ln T$	[49]
	$G^{Al_3Zr_2}_{Cu:Zr} = 0.25G^{Cu_2Zr}_{Cu:Zr}+0.25G^{Cu_{10}Zr_7}_{Cu:Zr}+25000.0$	This work
AlZr: $(Al,Cu)Zr$	$G^{AlZr}_{Al:Zr} = GHSER_{Al}+GHSER_{Zr}-88030.8-58.1780T+8.8000T\ln T$	[49]
	$G^{AlZr}_{Cu:Zr} = G^{CuZr}_{Cu:Zr}+10000.0$	This work
	${}^0L^{AlZr}_{Al,Cu:Zr} = +10920.1-40.0104T$	This work
Al_4Zr_5: $(Al,Cu)_4Zr_5$	$G^{Al_4Zr_5}_{Al:Zr} = 4GHSER_{Al}+5GHSER_{Zr}-336727.1-293.7755T+39.6000T\ln T$	[49]
	$G^{Al_4Zr_5}_{Cu:Zr} = 1.5G^{CuZr}_{Cu:Zr}+0.5G^{Cu_5Zr_7}_{Cu:Zr}+45000.0$	This work
	${}^0L^{Al_4Zr_5}_{Al,Cu:Zr} = +255951.1-150.0000T$	This work
	${}^1L^{Al_4Zr_5}_{Al,Cu:Zr} = -144050.2-150.0000T$	This work
Al_3Zr_4: $(Al,Cu)_3Zr_4$	$G^{Al_3Zr_4}_{Al:Zr} = 3GHSER_{Al}+4GHSER_{Zr}-277084.9-213.3937T+30.8000T\ln T$	[49]
	$G^{Al_3Zr_4}_{Cu:Zr} = 0.5G^{CuZr}_{Cu:Zr}+0.5G^{Cu_5Zr_7}_{Cu:Zr}+35000.0$	This work
	${}^0L^{Al_3Zr_4}_{Al,Cu:Zr} = -115951.1+150.0000T$	This work
	${}^1L^{Al_3Zr_4}_{Al,Cu:Zr} = -470952.3+150.0000T$	This work
Al_2Zr_3: $(Al,Cu)_2Zr_3$	$G^{Al_2Zr_3}_{Al:Zr} = 2GHSER_{Al}+3GHSER_{Zr}-187717.0-155.8703T+22.0000T\ln T$	[49]
	$G^{Al_2Zr_3}_{Cu:Zr} = 0.3333G^{Cu_5Zr_7}_{Cu:Zr}+0.3333G^{CuZr_2}_{Cu:Zr}+25000.0$	This work
Al_3Zr_5: $(Al,Cu)_3Zr_5$	$G^{Al_3Zr_5}_{Al:Zr} = 3GHSER_{Al}+5GHSER_{Zr}-282402.4-252.0107T+35.2000T\ln T$	[49]
	$G^{Al_3Zr_5}_{Cu:Zr} = 0.3333G^{Cu_5Zr_7}_{Cu:Zr}+1.3333G^{CuZr_2}_{Cu:Zr}+40000.0$	This work
$AlZr_2$: $(Al,Cu)Zr_2$	$G^{AlZr_2}_{Al:Zr} = GHSER_{Al}+2GHSER_{Zr}-104004.0-88.9112T+13.2000T\ln T$	[49]
	$G^{AlZr_2}_{Cu:Zr} = G^{CuZr_2}_{Cu:Zr}+15000.0$	This work
	${}^0L^{AlZr_2}_{Al,Cu:Zr} = +29325.1-25.1021T$	This work
$AlZr_3$: $(Al,Cu)Zr_3$	$G^{AlZr_3}_{Al:Zr} = GHSER_{Al}+3GHSER_{Zr}-110728.0-116.1706T+17.6000T\ln T$	[49]
	$G^{AlZr_3}_{Cu:Zr} = G^{CuZr_2}_{Cu:Zr}+GHSER_{Zr}+20000.0$	This work
	${}^0L^{AlZr_3}_{Al,Cu:Zr} = -21988.9$	This work
Cu_9Zr_2: $Cu_9(Al,Zr)_2$	$G^{Cu_9Zr_2}_{Cu:Al} = 2.3043GHSER_{Cu}+8.6957G^{\alpha_2}_{Al:Cu}+55000.0$	This work
	$G^{Cu_9Zr_2}_{Cu:Zr} = 9GHSER_{Cu}+2GHSER_{Zr}-103514.6-4.5000T$	[57]
$Cu_{51}Zr_{14}$: $(Al,Cu)_{51}Zr_{14}$	$G^{Cu_{51}Zr_{14}}_{Al:Zr} = 9GHSER_{Al}+14G^{Al_3Zr}_{Al:Zr}+325000.0$	This work
	$G^{Cu_{51}Zr_{14}}_{Cu:Zr} = 51GHSER_{Cu}+14GHSER_{Zr}-661977.0-66.6900T$	[57]
	${}^0L^{Cu_{51}Zr_{14}}_{Al,Cu:Zr} = -2000201.2$	This work
	${}^1L^{Cu_{51}Zr_{14}}_{Al,Cu:Zr} = +1000155.4$	This work
Cu_8Zr_3: $(Al,Cu)_8Zr_3$	$G^{Cu_8Zr_3}_{Al:Zr} = 2G^{Al_2Zr}_{Al:Zr}+G^{Al_3Zr}_{Al:Zr}+55000.0$	This work
	$G^{Cu_8Zr_3}_{Cu:Zr} = 8GHSER_{Cu}+3GHSER_{Zr}-131178.7-4.8278T$	[57]
Cu_2Zr: $(Al,Cu)_2Zr$	$G^{Cu_2Zr}_{Al:Zr} = G^{Al_2Zr}_{Al:Zr}+15000.0$	This work
	$G^{Cu_2Zr}_{Cu:Zr} = 2GHSER_{Cu}+GHSER_{Zr}-34276.4-4.4265T$	[57]
$Cu_{10}Zr_7$: $(Al,Cu)_{10}Zr_7$	$G^{Cu_{10}Zr_7}_{Al:Zr} = 3G^{Al_2Zr_3}_{Al:Zr}+G^{AlZr}_{Al:Zr}+85000.0$	This work
	$G^{Cu_{10}Zr_7}_{Cu:Zr} = 10GHSER_{Cu}+7GHSER_{Zr}-347872.9+100.0025T$	[57]
CuZr: $(Al,Cu)Zr$	$G^{CuZr}_{Al:Zr} = G^{AlZr}_{Al:Zr}+10000.0$	This work
	$G^{CuZr}_{Cu:Zr} = GHSER_{Cu}+GHSER_{Zr}-29672.1+1.7174T$	[57]
	${}^0L^{CuZr}_{Al,Cu:Zr} = -20101.2$	This work
Cu_5Zr_7: $(Al,Cu)_5Zr_7$	$G^{Cu_5Zr_7}_{Al:Zr} = G^{Al_3Zr_4}_{Al:Zr}+G^{Al_2Zr_3}_{Al:Zr}+60000.0$	This work
	$G^{Cu_5Zr_7}_{Cu:Zr} = 5GHSER_{Cu}+7GHSER_{Zr}-182235.0+21.7236T$	[57]
$CuZr_2$: $(Al,Cu)Zr_2$	$G^{CuZr_2}_{Al:Zr} = G^{AlZr_2}_{Al:Zr}+15000.0$	This work
	$G^{CuZr_2}_{Cu:Zr} = GHSER_{Cu}+2GHSER_{Zr}-51135.3+12.8805T$	[57]
	${}^0L^{CuZr_2}_{Al,Cu:Zr} = -15889.1$	This work
	${}^1L^{CuZr_2}_{Al,Cu:Zr} = +9988.5$	This work
τ_1: $Al_{14}Cu_{71}Zr_{15}$	$G^{\tau_1}_{Al:Cu:Zr} = 14GHSER_{Al}+71GHSER_{Cu}+15GHSER_{Zr}-3673010.1+998.9112T$	This work
τ_2: $Al_3Cu_6Zr_{16}$	$G^{\tau_2}_{Al:Cu:Zr} = 3GHSER_{Al}+6GHSER_{Cu}+16GHSER_{Zr}-353590.2-169.8597T$	This work
τ_3:$(Al,Cu)Zr$	$G^{\tau_3}_{Al:Zr} = G^{AlZr}_{Al:Zr}+10000.0$	This work
	$G^{\tau_3}_{Cu:Zr} = G^{CuZr}_{Cu:Zr}+10000.0$	This work
	${}^0L^{\tau_3}_{Al,Cu:Zr} = -45540.8-19.9857T$	This work
τ_4: $AlCu_2Zr$	$G^{\tau_4}_{Al:Cu:Zr} = GHSER_{Al}+2GHSER_{Cu}+GHSER_{Zr}-193921.0+40.1002T$	This work
τ_6: Al_3Cu_4Zr	$G^{\tau_6}_{Al:Cu:Zr} = 3GHSER_{Al}+4GHSER_{Cu}+GHSER_{Zr}-261134.3-5.0013T$	This work

(*continued on next page*)

Table 2 (*continued*)

Phase	Thermodynamic parameters	Reference
τ_7: $(Al,Cu)_{12}Zr$	$G^{\tau_7}_{Al:Zr} = 9GHSER_{Al} + G^{Al_3Zr}_{Al:Zr} + 65000.0$	This work
	$G^{\tau_7}_{Cu:Zr} = 7.5GHSER_{Cu} + 0.5G^{Cu_9Zr_2}_{Cu:Zr} + 65000.0$	This work
	${}^0L^{\tau_7}_{Al,Cu:Zr} = -1090120.2$	This work
	${}^1L^{\tau_7}_{Al,Cu:Zr} = -81924.2 + 300.0011T$	This work
	${}^2L^{\tau_7}_{Al,Cu:Zr} = +1002142.4$	This work
τ_9: $Al_{68}Cu_{15}Zr_{17}$	$G^{\tau_9}_{Al:Cu:Zr} = 68GHSER_{Al} + 15GHSER_{Cu} + 17GHSER_{Zr} - 3914083.4 + 470.9891T$	This work
τ_{11}: $Al_{13}Cu_{79}Zr_8$	$G^{\tau_{11}}_{Al:Cu:Zr} = 13GHSER_{Al} + 79GHSER_{Cu} + 8GHSER_{Zr} - 1017161.1 - 643.1121T$	This work
Al_3Zr, τ_8: $(Al,Cu)_3Zr$	$G^{M_3Zr}_{Al:Zr} = 3GHSER_{Al} + GHSER_{Zr} - 182476.0 - 89.2872T + 15.5760T\ \ln T$	[49]
	$G^{M_3Zr}_{Cu:Zr} = 3GHSER_{Cu} + GHSER_{Zr} - 44941.1 - 2.6863T + 20000$	This work
	${}^1L^{M_3Zr}_{Al,Cu:Zr} = -572978.0 + 21.9640T$	This work
	${}^2L^{M_3Zr}_{Al,Cu:Zr} = +442254.8 + 26.4001T$	This work

[a] In SI units (Joule, mole of the formula units and Kelvin).

Table 3
Invariant reactions in the Al–Cu–Zr system.

Reaction	Type[a,b]	Present work			
		T (K)	Composition		
			x(Al)	x(Cu)	x(Zr)
liq. + Al_4Zr_5 + Al_3Zr_2	C_1	1756	0.5065	0.0050	0.4885
liq. + Al_4Zr_5 + AlZr	C_2	1534	0.3255	0.1896	0.4850
liq. + Al_4Zr_5 + τ_3	C_3	1531	0.3037	0.1873	0.5090
liq. + AlZr + τ_3	C_4	1529	0.3097	0.1893	0.5010
liq. + τ_4 + Al_2Zr	C_5	1523	0.2685	0.4593	0.2721
liq. + τ_3 + Al_2Zr	C_6	1508	0.3063	0.2494	0.4443
liq. + τ_2 + bcc	C_7	1499	0.0970	0.1867	0.7162
liq. + τ_6 + Al_2Zr	C_8	1498	0.3972	0.4270	0.1458
liq. + τ_3 + τ_2	C_9	1496	0.1674	0.2653	0.5673
liq. + τ_6 + τ_7	C_{10}	1488	0.4024	0.5139	0.0837
liq. + τ_4 + $Cu_{51}Zr_{14}$	C_{11}	1484	0.1415	0.6442	0.2143
liq. + τ_{11} + τ_4	C_{12}	1477	0.1752	0.6923	0.1326
liq. + $Cu_{51}Zr_{14}$ + τ_{11}	C_{13}	1471	0.1117	0.7281	0.1601
liq. + Cu_9Zr_2 + $Cu_{51}Zr_{14}$	C_{14}	1339	0.0180	0.8687	0.1133
liq. + τ_{11} + fcc	C_{15}	1327	0.1259	0.8662	0.0078
liq. + $CuZr_2$ + τ_2	C_{16}	1317	0.0173	0.3125	0.6702
liq. + τ_6 + bcc	C_{17}	1300	0.2593	0.7299	0.0108
liq. + τ_1 + bcc	C_{18}	1296	0.1956	0.7919	0.0125
liq. + τ_{11} + bcc	C_{19}	1295	0.1849	0.8046	0.0105
liq. + bcc + τ_4	C_{20}	1292	0.2253	0.7561	0.0187
liq. + CuZr + τ_3	C_{21}	1253	0.0175	0.4889	0.4936
$AlZr_2$ + bcc + $AlZr_3$	C_{22}	1479	0.1660	0.0474	0.7866
bcc + τ_7 + ε_2	C_{23}	1122	0.4625	0.4606	0.0769
τ_7 + δ_1 + γ_1	C_{24}	958	0.4711	0.4520	0.0769
τ_7 + δ_1 + ε_2	C_{25}	958	0.4711	0.4520	0.0769
τ_7 + ε_2 + ζ	C_{26}	871	0.5104	0.4127	0.0769
liq. + Al_3Zr_2 → Al_2Zr + Al_4Zr_5	U_1	1666	0.4908	0.0671	0.4422
liq. + Al_2Zr_3 → Al_3Zr_5 + Al_4Zr_5	U_2	1644	0.3211	0.0062	0.6727
liq. + Al_3Zr + Al_2Zr → τ_8	P_1	1639	0.6657	0.1359	0.1983
liq. + Al_3Zr_5 → bcc + Al_4Zr_5	U_3	1570	0.2893	0.0206	0.6901
liq. → AlZr + Al_4Zr_5 + τ_3	E_1	1529	0.3097	0.1893	0.5010
liq. + Al_4Zr_5 → Al_2Zr + AlZr	U_4	1528	0.3613	0.1836	0.4551
liq. → Al_2Zr + AlZr + τ_3	E_2	1505	0.3284	0.2127	0.4589
liq. + Al_2Zr → τ_4 + τ_6	U_5	1471	0.3173	0.5230	0.1597
liq. → $Cu_{51}Zr_{14}$ + τ_4 + τ_{11}	E_3	1466	0.1408	0.6961	0.1630
liq. + τ_6 → Al_2Zr + τ_7	U_6	1429	0.4809	0.3817	0.1374
liq. + Al_2Zr → τ_7 + τ_8	U_7	1426	0.4867	0.3771	0.1363
bcc + Al_4Zr_5 → liq. + $AlZr_2$	U_8	1369	0.2359	0.1049	0.6591
$Cu_{51}Zr_{14}$ + τ_{11} → liq. + τ_1	U_9	1364	0.0468	0.8501	0.1031
τ_4 + τ_{11} → liq. + τ_1	U_{10}	1335	0.2081	0.7648	0.0272
liq. + $Cu_{51}Zr_{14}$ → τ_1 + Cu_9Zr_2	U_{11}	1334	0.0344	0.8683	0.0973
liq. + Al_4Zr_5 → $AlZr_2$ + τ_3	U_{12}	1317	0.2298	0.1325	0.6377
liq. + τ_2 → $CuZr_2$ + bcc	U_{13}	1315	0.0180	0.2826	0.6994
liq. + τ_{11} → fcc + τ_1	U_{14}	1311	0.0547	0.9057	0.0396
liq. + τ_6 → τ_7 + bcc	U_{15}	1296	0.2951	0.6979	0.0070
liq. → τ_{11} + bcc + fcc	E_4	1295	0.1849	0.8046	0.0105
liq. + bcc → τ_2 + $AlZr_2$	U_{16}	1295	0.2124	0.1368	0.6508
liq. → τ_1 + τ_{11} + bcc	E_5	1295	0.1886	0.7999	0.0114
liq. → $AlZr_2$ + τ_3 + τ_2	E_6	1295	0.2143	0.1381	0.6477
liq. → bcc + τ_4 + τ_1	E_7	1292	0.2243	0.7571	0.0186

Table 3 (*continued*)

Reaction	Type[a,b]	Present work			
		T (K)	Composition		
			x(Al)	x(Cu)	x(Zr)
liq. → τ_6 + bcc + τ_4	E_8	1292	0.2301	0.7510	0.0189
liq. + τ_1 → fcc + Cu_9Zr_2	U_{17}	1284	0.0285	0.9058	0.0657
liq. + bcc → τ_7 + γ_2	U_{18}	1283	0.3284	0.6676	0.0040
liq. + τ_2 → τ_3 + $CuZr_2$	U_{19}	1280	0.0249	0.4009	0.5742
liq. + Cu_8Zr_3 → Cu_2Zr + $Cu_{51}Zr_{14}$	U_{20}	1251	0.0021	0.6442	0.3537
liq. + τ_3 → CuZr + $CuZr_2$	U_{21}	1242	0.0159	0.4424	0.5416
liq. + τ_3 → Al_2Zr + CuZr	U_{22}	1233	0.0195	0.5345	0.4460
liq. + $CuZr_2$ → CuZr + Cu_5Zr_7	U_{23}	1229	0.0062	0.4537	0.5401
liq. + γ_2 → τ_7 + bcc	U_{24}	1225	0.4017	0.5966	0.0018
liq. + $Cu_{51}Zr_{14}$ → τ_4 + Cu_2Zr	U_{25}	1212	0.0109	0.6003	0.3888
liq. + Al_2Zr → CuZr + τ_4	U_{26}	1191	0.0104	0.5732	0.4165
liq. + τ_4 → CuZr + Cu_2Zr	U_{27}	1181	0.0089	0.5800	0.4111
liq. → CuZr + Cu_2Zr + $Cu_{10}Zr_7$	E_9	1180	0.0045	0.5800	0.4165
τ_7 + bcc → liq. + ε_2	U_{28}	1120	0.4829	0.5160	0.0011
liq. + τ_8 → τ_7 + Al_3Zr	U_{29}	1111	0.6587	0.2992	0.0421
liq. + τ_8 → τ_7 + Al_3Zr	U[b]	1093	–	–	–
liq. + τ_7 + Al_3Zr → τ_9	P_2	1011	0.6871	0.2865	0.0263
liq. + τ_7 + Al_3Zr → τ_9	P[b]	1013	–	–	–
liq. + ε_2 → τ_7 + η_1	U_{30}	897	0.6559	0.3415	0.0026
liq. + η_1 → θ + τ_7	U_{31}	865	0.6833	0.3134	0.0033
liq. + τ_7 → τ_9 + θ	U_{32}	856	0.7262	0.2651	0.0087
liq. + Al_3Zr → fcc + τ_9	U_{33}	823	0.8216	0.1715	0.0069
liq. → fcc + τ_9 + θ	E_{10}	818	0.8155	0.1779	0.0066
Al_3Zr_5 + bcc → $AlZr_2$ + Al_4Zr_5	U_{34}	1481	0.2124	0.0111	0.7765
Al_4Zr_5 + Al_3Zr_2 + Al_2Zr → AlZr	P_3	1445	0.4838	0.0162	0.5000
τ_4 + $Cu_{51}Zr_{14}$ + τ_{11} → τ_1	P_4	1422	0.1300	0.7900	0.0800
AlZr → Al_4Zr_5 + τ_3 + Al_2Zr	E_{11}	1414	0.3785	0.0659	0.5556
$AlZr_2$ + Al_4Zr_5 + Al_3Zr_5 → Al_3Zr_4	P_5	1331	0.3310	0.0023	0.6667
Al_3Zr_5 + Al_4Zr_5 → Al_3Zr_4 + Al_2Zr_3	U_{35}	1331	0.3998	0.0447	0.5556
$AlZr_2$ + Al_4Zr_5 → Al_3Zr_4 + τ_3	U_{36}	1313	0.2302	0.1295	0.6403
Al_3Zr_4 + Al_3Zr_5 → $AlZr_2$ + Al_2Zr_3	U_{37}	1310	0.3318	0.0015	0.6667
τ_{11} + bcc → fcc + τ_1	U_{38}	1292	0.1400	0.7100	0.1500
bcc + $AlZr_2$ → $AlZr_3$ + τ_2	U_{39}	1292	0.1377	0.0476	0.8148
Al_4Zr_5 + τ_3 → Al_2Zr + Al_3Zr_4	U_{40}	1286	0.3833	0.0612	0.5556
τ_2 + $AlZr_2$ → $AlZr_3$ + τ_3	U_{41}	1280	0.2594	0.2406	0.5000
τ_3 + $AlZr_2$ → Al_3Zr_4 + $AlZr_3$	U_{42}	1260	0.3606	0.0680	0.5714
Al_4Zr_5 → Al_2Zr + AlZr + Al_3Zr_4	E_{12}	1256	0.4811	0.0189	0.5000
τ_4 + bcc → τ_1 + τ_6	U_{43}	1252	0.3750	0.5000	0.1250
τ_7 + bcc → γ_2 + τ_6	U_{44}	1244	0.3864	0.5366	0.0769
τ_2 + bcc → $AlZr_3$ + $CuZr_2$	U_{45}	1204	0.1913	0.0587	0.7500
$AlZr_3$ + τ_2 → τ_3 + $CuZr_2$	U_{46}	1191	0.2413	0.2587	0.5000
Cu_2Zr + CuZr → $Cu_{10}Zr_7$ + τ_4	U_{47}	1175	0.0190	0.4810	0.5000
τ_4 + $Cu_{51}Zr_{14}$ → Cu_2Zr + τ_1	U_{48}	1160	0.0016	0.6651	0.3333
τ_3 + $AlZr_3$ → Al_3Zr_4 + $CuZr_2$	U_{49}	1152	0.3510	0.0776	0.5714
bcc + γ_2 → τ_7 + γ_1	U_{50}	1146	0.4530	0.4701	0.0769
Cu_2Zr + τ_4 → $Cu_{10}Zr_7$ + τ_1	U_{51}	1138	0.0014	0.6653	0.3333
Cu_2Zr + $Cu_{51}Zr_{14}$ → τ_1 + Cu_8Zr_3	U_{52}	1126	0.0008	0.6659	0.3333
bcc → τ_7 + ε_2 + γ_1	E_{13}	1122	0.4615	0.4616	0.0769
τ_7 + Al_2Zr → τ_6 + τ_8	U_{53}	1114	0.3750	0.5000	0.1250
Cu_2Zr → τ_1 + Cu_8Zr_3 + $Cu_{10}Zr_7$	E_{14}	1113	0.0007	0.6660	0.3333
τ_7 + γ_2 → γ_1 + τ_6	U_{54}	1103	0.3750	0.5000	0.1250
bcc + $AlZr_3$ → hcp + $CuZr_2$	U_{55}	1099	0.1874	0.0626	0.7500
τ_3 + CuZr → Al_2Zr + $CuZr_2$	U_{56}	1075	0.2391	0.4276	0.3333
γ_2 + τ_6 → γ_1 + bcc	U_{57}	1064	0.3750	0.5000	0.1250
CuZr + Al_2Zr → τ_4 + $CuZr_2$	U_{58}	1008	0.2334	0.4333	0.3333
τ_3 → Al_2Zr + Al_3Zr_4 + $CuZr_2$	E_{15}	1000	0.3221	0.3445	0.3333
bcc + τ_6 → τ_1 + γ_1	U_{59}	994	0.3750	0.5000	0.1250
CuZr+Cu_5Zr_7 → $Cu_{10}Zr_7$ + $CuZr_2$	U_{60}	993	0.0009	0.3324	0.6667
CuZr → $Cu_{10}Zr_7$ + τ_4 + $CuZr_2$	E_{16}	970	0.0195	0.3138	0.6667
τ_7 + δ_1 → ε_2 + γ_1	U_{61}	958	0.4711	0.4520	0.0769
$Cu_{10}Zr_7$+$Cu_{51}Zr_{14}$ → τ_1 + Cu_8Zr_3	U_{62}	887	0.1400	0.7100	0.1500
τ_7 + η_1 + ε_2 → η_2	P_6	871	0.5376	0.3855	0.0769
τ_7 + ε_2 → ζ + η_2	U_{63}	854	0.5344	0.3887	0.0769
τ_7 + γ_1 → τ_6 + δ_1	U_{64}	848	0.3750	0.5000	0.1250
τ_7 + η_1 → η_2 + θ	U_{65}	847	0.5470	0.3761	0.0769
τ_1 + bcc → fcc + γ_1	U_{66}	841	0.1400	0.7100	0.1500
τ_7 + ε_2 → ζ + δ_1	U_{67}	831	0.4916	0.4314	0.0769
τ_7 + θ → η_2 + τ_9	U_{68}	771	0.5497	0.3734	0.0769
fcc + τ_9 → θ + Al_3Zr	U_{69}	767	0.9849	0.0150	0.0001
τ_7 + Al_3Zr → τ_8 + τ_9	U_{70}	765	0.6773	0.0727	0.2500
τ_7 + η_2 → τ_9 + ζ	U_{71}	739	0.5329	0.3902	0.0769
τ_6 + τ_7 → τ_8 + δ_1	U_{72}	710	0.3750	0.5000	0.1250
τ_7 + τ_9 → τ_8 + ζ	U_{73}	680	0.6647	0.0853	0.2500

Table 3 (*continued*)

Reaction	Type[a,b]	Present work			
		T (K)	Composition		
			x(Al)	x(Cu)	x(Zr)
$\tau_7 \rightarrow \tau_8 + \delta_1 + \zeta$	E_{17}	673	0.6447	0.1053	0.2500
$\tau_6 + \tau_8 \rightarrow Al_2Zr + \delta_1$	U_{74}	666	0.3750	0.5000	0.1250
$\gamma_1 + fcc \rightarrow \tau_1 + \alpha_2$	U_{75}	636	0.1400	0.7100	0.1500
$\gamma_1 + \tau_6 \rightarrow \tau_1 + \delta_1$	U_{76}	631	0.3750	0.5000	0.1250
$\tau_1 + \tau_6 \rightarrow \delta_1 + \tau_4$	U_{77}	586	0.3750	0.5000	0.1250
$Cu_{51}Zr_{14} \rightarrow \tau_1 + Cu_{10}Zr_7 + Cu_9Zr_2$	E_{18}	547	0.1400	0.7100	0.1500
$\tau_6 \rightarrow \delta_1 + \tau_4 + Al_2Zr$	E_{19}	507	0.3274	0.3393	0.3333
$Al_2Zr + CuZr_2 \rightarrow Al_3Zr_4 + \tau_4$	U_{78}	395	0.3274	0.3393	0.3333
$Al_2Zr + AlZr \rightarrow Al_3Zr_2 + Al_3Zr_4$	U_{79}	387	0.5905	0.0762	0.3333
$\tau_8 + \zeta \rightarrow \delta_1 + \tau_9$	U_{80}	364	0.6638	0.0862	0.2500

[a] C: Congruent melting, E: Eutectic or Eutectoid reaction, P: Peritectic or Peritectoid reaction, U: Quasi-peritectic or Quasi-peritectoid reaction.
[b] They were determined by Soares and Castro [64].

parameters of the phases γ_1 and liquid were modified by Witusiewicz et al. [35]. Recently, the thermodynamic description of the Al–Cu system has been carried out by Liang and Schmid-Fetzer [36]. It is the first time that all available experimental data have been consistent with the calculated results [36], so their optimized results have been adopted in the present work. Fig. 1 represents the calculated Al–Cu phase diagram.

2.2. Al–Zr system

The thermodynamic assessment of the Al–Zr system was firstly carried out by Saunders and Rivlin [37] and then revised by Saunders [38]. In their work [37,38], the compound Al_3Zr_4 was not considered. Later, the enthalpies of formation of the compounds Al_2Zr and Al_3Zr were measured by several researchers [39,40] and the phase diagram of the Zr-rich part in the Al–Zr system was re-determined by Peruzzi [41]. According to the above experimental information, the Al–Zr system was re-optimized by Wang et al. [42]. Their calculated enthalpies of formation of the compounds were very negative and the compound AlZr had a minimum value. However, the enthalpies of formation of the compounds [43–48] were calculated using first-principles calculations and all results showed that the compound Al_2Zr had a minimum value. To match the calculated results [43–48], Fischer and Colinet [49] have carried out a new thermodynamic modeling of the Al–Zr system, which is accepted in the present work. Fig. 2 shows the calculated Al–Zr phase diagram.

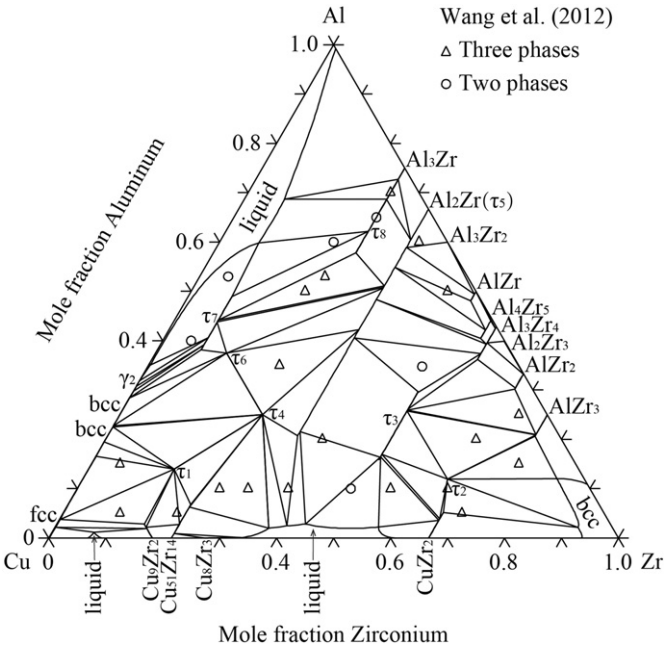

Fig. 5. Calculated isothermal section of the Al–Cu–Zr system at 1273 K compared with the experimental data [69].

2.3. Cu–Zr system

To improve the enthalpies of formation of the compounds in the Cu-rich part [50], Zeng and Hämäläinen [51] re-assessed the Cu–Zr system. He et al. [52] adopt the same parameters as [51] except the compound CuZr to evaluating the Ag–Cu–Zr system. Due to short-range-order in

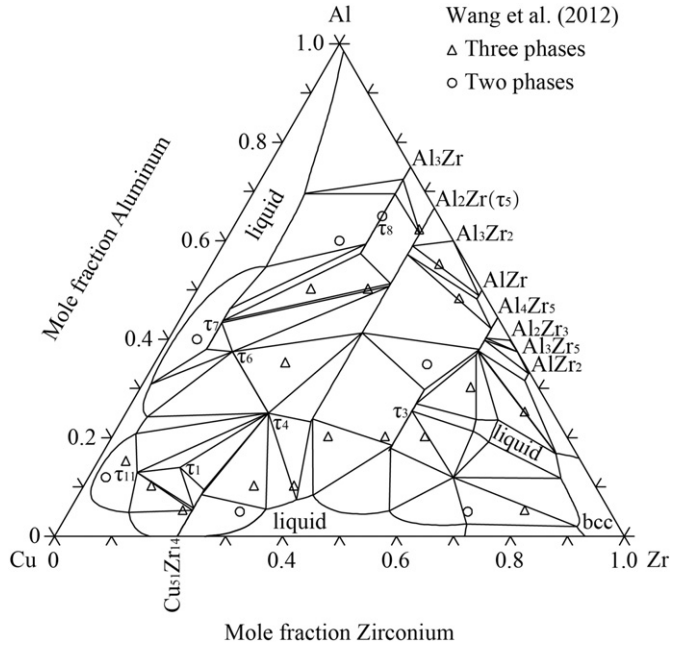

Fig. 4. Calculated isothermal section of the Al–Cu–Zr system at 1373 K compared with the experimental data [69].

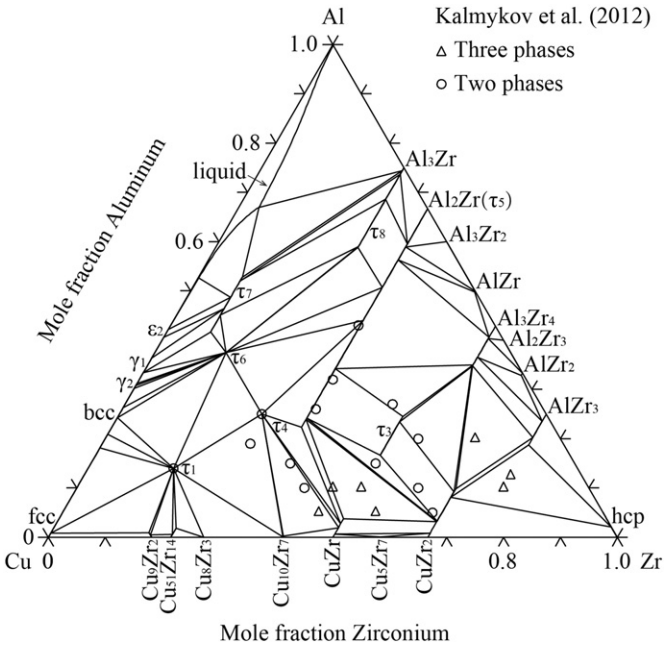

Fig. 6. Calculated isothermal section of the Al–Cu–Zr system at 1073 K compared with the experimental data [70].

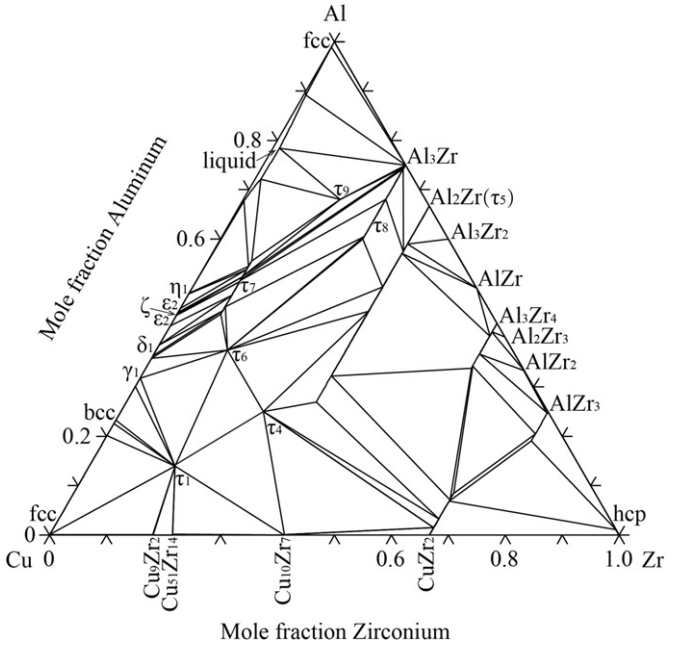

Fig. 7. Calculated isothermal section of the Al–Cu–Zr system at 873 K.

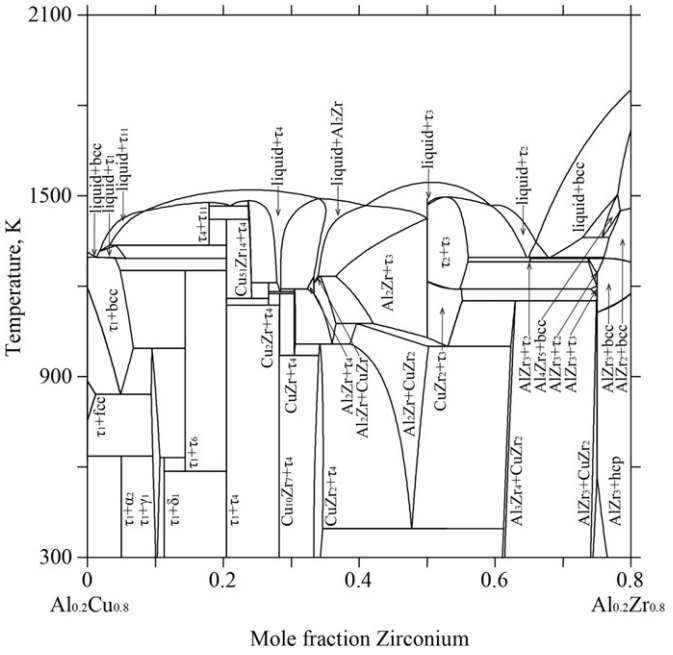

Fig. 9. Calculated vertical section of the Al–Cu–Zr system at 20 at.% Al.

liquid, Abe et al. [53] used an associated solution model to assess the Cu–Zr system. Later, the Cu–Zr system was re-optimized by Wang et al. [54] and the liquid phase was first treated as the substitutional model with temperature independence. Then, Yamaguchi et al. [55] determined the heat contents of the Cu–Zr alloys in the temperature range from 880 to 1470 K using drop calorimetry and measured the enthalpies of mixing of the liquid phase at 1443 K using high temperature calorimetry. Based their own experimental data [55], the thermodynamic description of the Cu–Zr system was performed. Kang and Jung [56] used the modified quasi-chemical model to describe the liquid phase, but the model was inappropriate to further assessments in the multicomponent system. Recently, the thermodynamic description of the Cu–Zr system has been evaluated previously by Gierlotka et al. [57]. For the first time, the enthalpies of mixing of the liquid phase have been comprehensively compared with calculated results [57] when the liquid phase is described as the substitutional solution model. The model could be easily extrapolated to the multicomponent system, therefore, their optimized results [57] have been adopted in the present work. Fig. 3 presents the calculated Cu–Zr phase diagram.

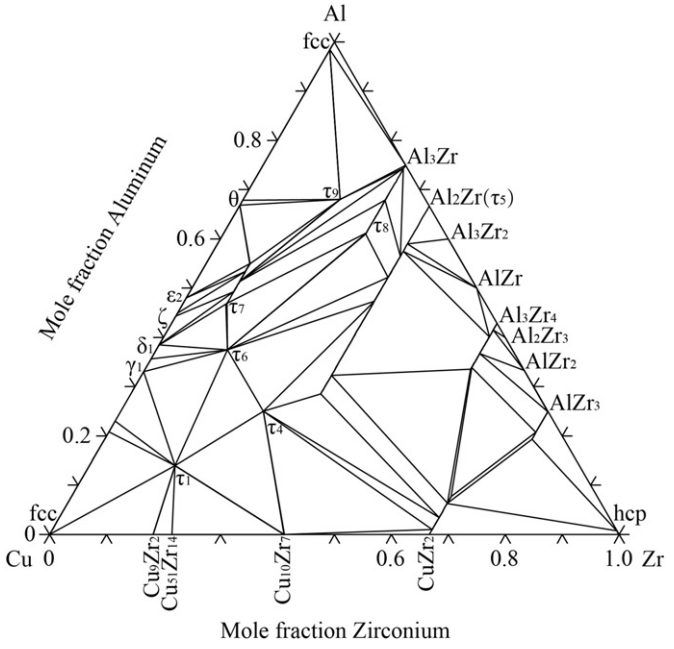

Fig. 8. Calculated isothermal section of the Al–Cu–Zr system at 773 K.

3. Experimental information on the Al–Cu–Zr system

The isothermal section at 673 K in the Al-rich side was measured by Zarechnyuk et al. [58], which was the first experimental information in the Al–Cu–Zr system. Using X-ray diffraction (XRD) and metallographic analysis, the isothermal sections at 1073 K across the whole range of

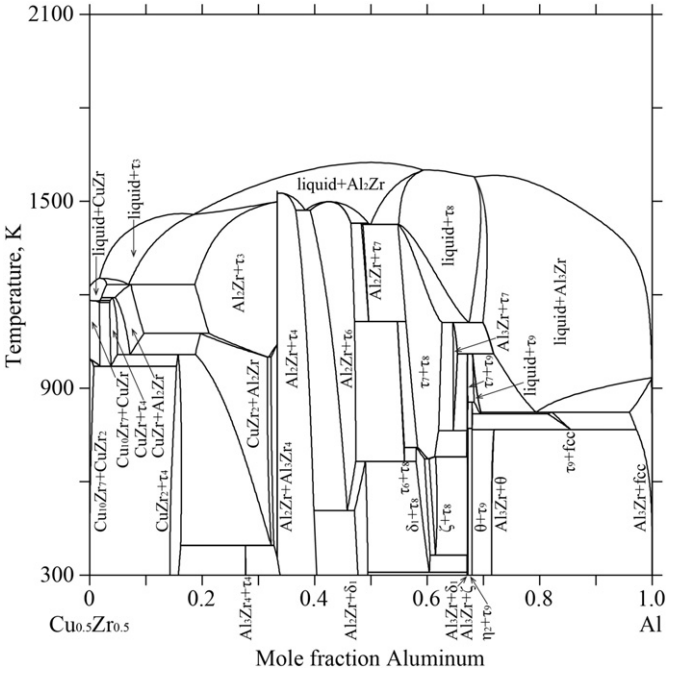

Fig. 10. Calculated vertical section of the Al–Cu–Zr system at a constant ratio of Cu:Zr = 1:1.

compositions and at 773 K in the Al-rich part were investigated by Markiv and Burnashova [59]. Eight ternary compounds τ_1, τ_2, τ_3, τ_4, τ_5, τ_6, τ_7 and τ_8 were reported to exist at 1073 K. One more compound τ_9' was detected at 773 K [59] but not observed at 673 K [58]. The crystal structures of only four ternary compounds τ_4, τ_5, τ_7 and τ_8 were determined. Furthermore, the ternary compounds of the Al–Cu–Zr system were investigated by Meyer et al. [60–62]. A new ternary compound $Al_7Cu_{16}Zr_6$ named τ_{10} was found, and two ternary compounds $Al_{14}Cu_{71}Zr_{15}$ named τ_1 and Al_3Cu_4Zr named τ_6 reported by Markiv and Burnashova [59] were confirmed. For the first time, the Al–Cu–Zr system has been reviewed concretely by Tretyachenko [63], who presented the isothermal section at 1073 K and two partial isothermal sections at 673 and 773 K in the Al-rich corner.

Using microstructure and differential thermal analysis (DTA), Soares and Castro [64] have determined the phase equilibria in the Al-rich part of the Al–Cu–Zr system. A new ternary compound τ_9 replacing τ_9' reported by Markiv and Burnashova [59] was found. The invariant reactions in the Al-rich corner were established: U-type reaction liq. $+ \tau_8 \rightarrow \tau_7 + Al_3Zr$ at 1093 $\pm$ 10 K and P-type reaction liq. $+ \tau_7 + Al_3Zr \rightarrow \tau_9$ at 1013 $\pm$ 10 K. Using high temperature calorimetry, the partial and integral enthalpies of mixing of liquid and undercooled liquid Al–Cu–Zr alloys at 1450 to 1485 K and 2010 to 2080 K have been measured by Witusiewicz et al. [65]. Based on the new experimental data [64,65], the Al–Cu–Zr system was re-summarized by Tretyachenko [66], who presented the isothermal section at 1073 K and five partial isothermal sections at 673, 773, 873, 973 and 1133 K in the Al-rich corner.

Thermodynamic analysis of the Al–Cu–Zr system was carried out by Bo et al. [67], who calculated the projection of liquidus surface and an isothermal section at 773 K. On the basis of the calculated results [67], Raghavan [68] reviewed the Al–Cu–Zr system at third time.

Recently, the isothermal sections at 1273 and 1373 K across the whole range of compositions in the Al–Cu–Zr system have been determined by Wang et al. [69] using XRD and electron probe microanalysis (EPMA). A new ternary compound named τ_{11} was firstly found at 1373 K in the Cu-rich corner. The isothermal section at 1073 K in the Zr-rich part was measured by Kalmykov et al. [70] using the same method as [69]. The solid solubilities of the third components for the partial compounds Al_3Zr, $CuZr_2$ and CuZr were different from that in the review [66], but the phase equilibria was in a good agreement. Moreover, the ternary compound τ_{10} reported by Meyer et al. [60–62] was not found.

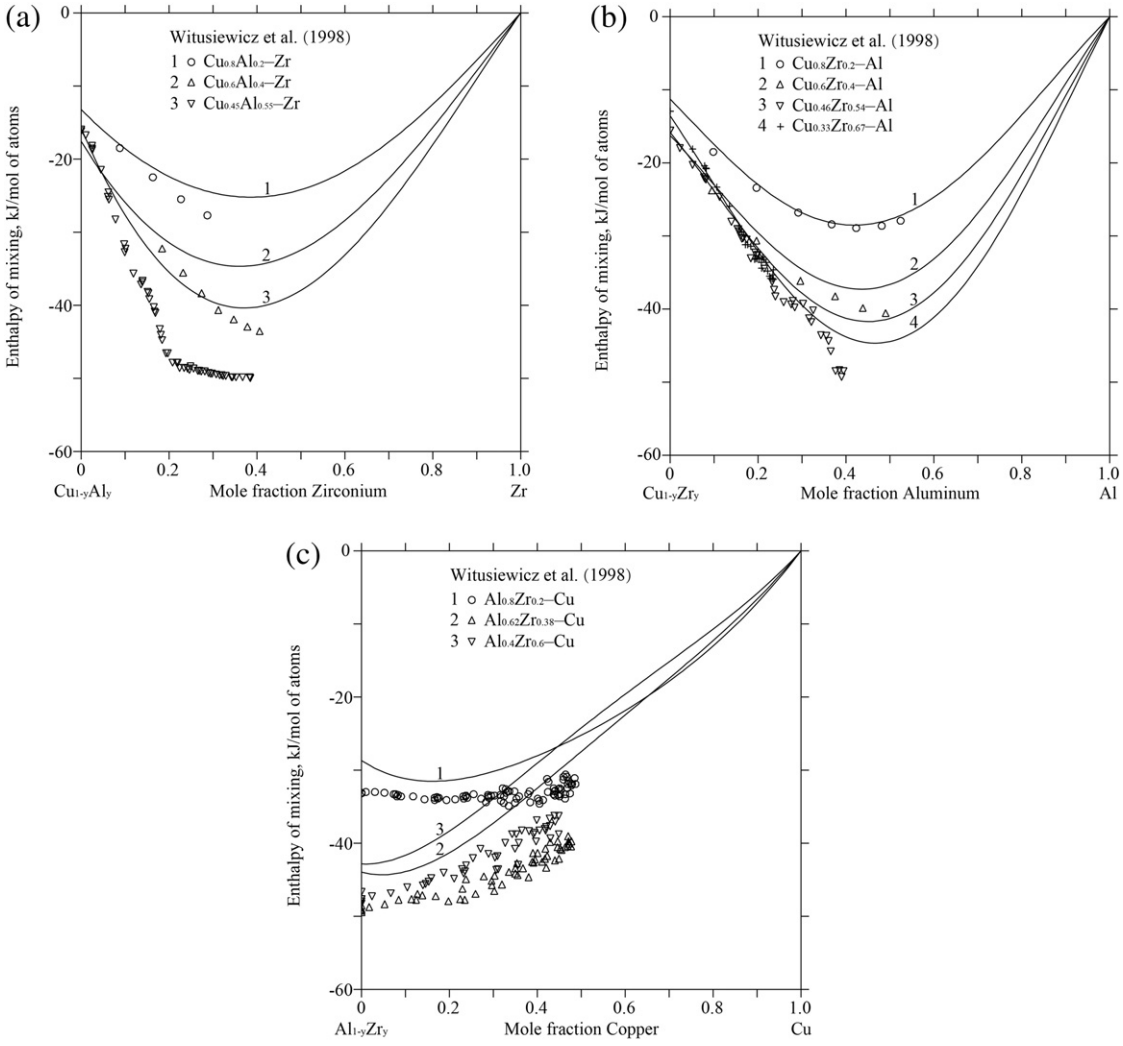

Fig. 11. a. Calculated enthalpies of mixing of ternary liquid and undercooled liquid Al–Cu–Zr alloys at 1450 K for 1 and 2, and 1485 K for 3 compared with the experimental data [65]. b. Calculated enthalpies of mixing of ternary liquid and undercooled liquid Al–Cu–Zr alloys at 1450 K for 1 and 2 and 1485 K for 3 and 4 compared with the experimental data [65]. c. Calculated enthalpies of mixing of ternary liquid and undercooled liquid Al–Cu–Zr alloys at 2045 $\pm$ 35 K compared with the experimental data [65].

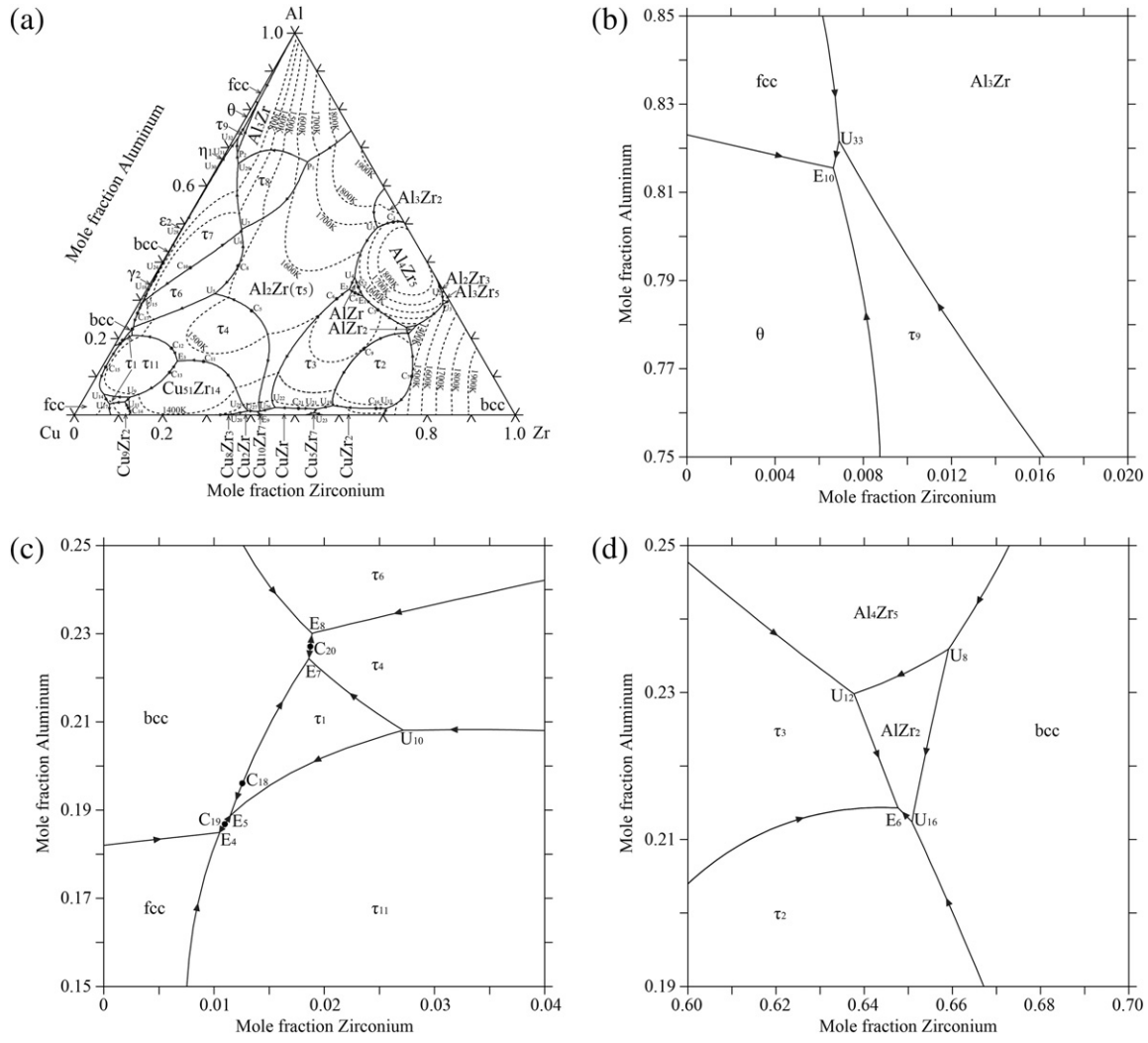

Fig. 12. a. Calculated projection of the liquidus surface in the Al–Cu–Zr system. b. Enlarged section of Fig. 12a. c. Enlarged section of Fig. 12a. d. Enlarged section of Fig. 12a.

Crystallographic description of the binary compounds in the Al–Zr and Cu–Zr systems and ternary compounds in the Al–Cu–Zr system is given in Table 1.

4. Thermodynamic models

4.1. Unary phases

In the SGTE database for pure elements [71], the Gibbs energy function is described by the following form:

$$G_i^{\phi}(T) = {}^{0}G_i^{\phi}(T) - H_i^{\mathrm{SER}}(298.15\ \mathrm{K}) = a + bT + cT\ \ln T + dT^2 + eT^{-1} + fT^3 + gT^7 + hT^{-9} \quad (1)$$

where H_i^{SER} represents the molar enthalpy of the element i (i = Al, Cu, Zr) at 298.15 K and 101,325 Pa in its standard element reference (SER) state, fcc for Al and Cu, and hcp for Zr. The molar Gibbs energy of the element i, $G_i^{\phi}(T)$, in its SER state, is denoted by GHSER_i, i.e.,

$$\mathrm{GHSER}_i = {}^{0}G_i^{\phi}(T) - H_i^{\mathrm{SER}}(298.15\ \mathrm{K}) \quad (2)$$

4.2. Solution phases

In the Al–Cu–Zr system, there are four solution phases liquid, fcc, bcc and hcp. Their molar Gibbs energy is expressed as the following form:

$$G_m^{\phi} = x_{\mathrm{Al}}G_{\mathrm{Al}}^{\phi} + x_{\mathrm{Cu}}G_{\mathrm{Cu}}^{\phi} + x_{\mathrm{Zr}}G_{\mathrm{Zr}}^{\phi} + RT(x_{\mathrm{Al}}\ \ln x_{\mathrm{Al}} + x_{\mathrm{Cu}}\ \ln x_{\mathrm{Cu}} + x_{\mathrm{Zr}}\ \ln x_{\mathrm{Zr}}) + {}^{E}G_m^{\phi} \quad (3)$$

where R is the gas constant; ${}^{E}G_m^{\phi}$ is the excess Gibbs energy and can be expressed as by the Redlich–Kister polynomial [72]:

$${}^{E}G_m^{\phi} = x_{\mathrm{Al}}x_{\mathrm{Cu}}\sum_j {}^{j}L_{\mathrm{Al,Cu}}^{\phi}(x_{\mathrm{Al}} - x_{\mathrm{Cu}})^j + x_{\mathrm{Al}}x_{\mathrm{Zr}}\sum_j {}^{j}L_{\mathrm{Al,Zr}}^{\phi}(x_{\mathrm{Al}} - x_{\mathrm{Zr}})^j + x_{\mathrm{Cu}}x_{\mathrm{Zr}}\sum_j {}^{j}L_{\mathrm{Cu,Zr}}^{\phi}(x_{\mathrm{Cu}} - x_{\mathrm{Zr}})^j + x_{\mathrm{Al}}x_{\mathrm{Cu}}x_{\mathrm{Zr}}{}^{j}L_{\mathrm{Al,Cu,Zr}}^{\phi} \quad (4)$$

where ${}^{j}L_{\mathrm{Al,Cu}}^{\phi}$, ${}^{j}L_{\mathrm{Al,Zr}}^{\phi}$ and ${}^{j}L_{\mathrm{Cu,Zr}}^{\phi}$ are the jth binary interaction parameters between elements Al and Cu, Al and Zr, and Cu and Zr, respectively; ${}^{j}L_{\mathrm{Al,Cu,Zr}}^{\phi}$ is the jth ternary interaction parameter to be

Fig. 13. a. Calculated invariant reaction scheme in the Al–Cu–Zr system. b. Calculated invariant reaction scheme in the Al–Cu–Zr system. c. Calculated invariant reaction scheme in the Al–Cu–Zr system. d. Calculated invariant reaction scheme in the Al–Cu–Zr system. e. Calculated invariant reaction scheme in the Al–Cu–Zr system. f. Calculated invariant reaction scheme in the Al–Cu–Zr system. g. Calculated invariant reaction scheme in the Al–Cu–Zr system.

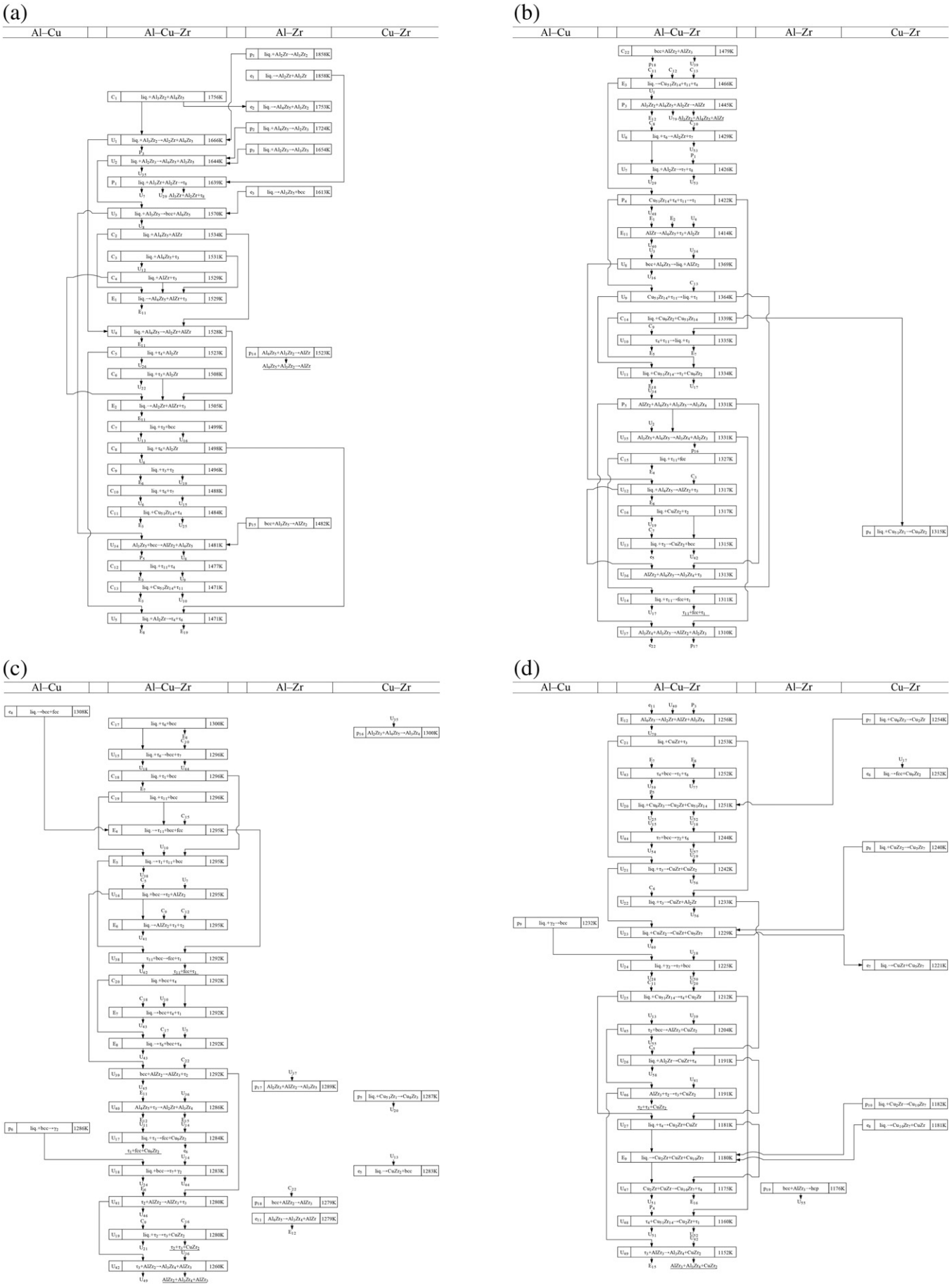
(a)
Al–Cu
Al–Cu–Zr
Al–Zr
Cu–Zr
(b)
Al–Cu
Al–Cu–Zr
Al–Zr
Cu–Zr
(c)
Al–Cu
Al–Cu–Zr
Al–Zr
Cu–Zr
(d)
Al–Cu
Al–Cu–Zr
Al–Zr
Cu–Zr

Fig. 13

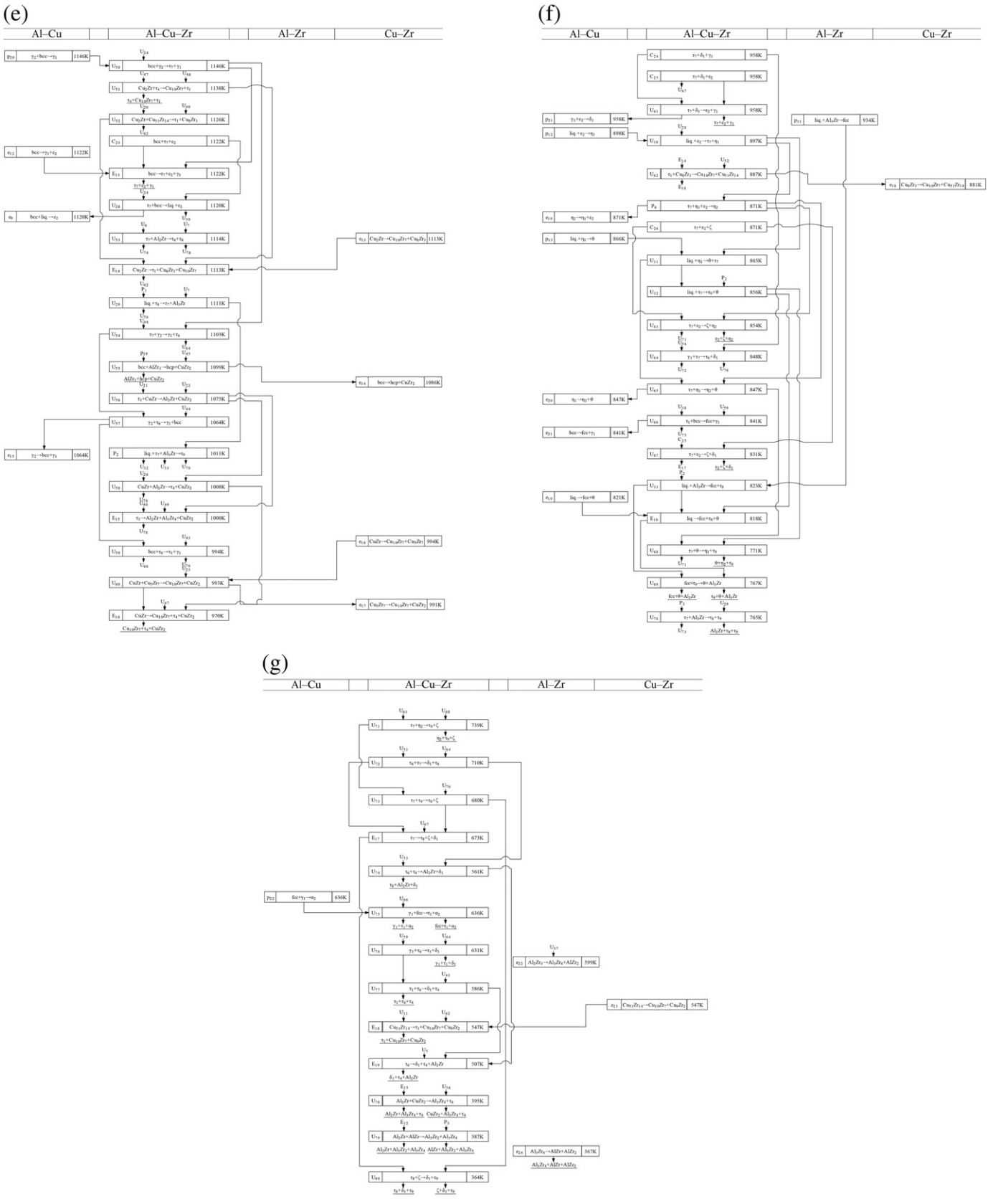

Fig. 13 (*continued*).

evaluated in this work, which in most cases is described as the following form:

$$ {}^{j}L^{\phi}_{\mathrm{Al,Cu,Zr}} = a_j + b_j T \tag{5} $$

where a_j and b_j are the parameters to be optimized in the present work.

4.3. The intermetallic compounds

In the Al–Zr and Cu–Zr systems, there are eighteen stoichiometric compounds, Al_3Zr, Al_2Zr, Al_3Zr_2, $AlZr$, Al_4Zr_5, Al_3Zr_4, Al_2Zr_3, Al_3Zr_5, $AlZr_2$, $AlZr_3$, Cu_9Zr_2, $Cu_{51}Zr_{14}$, Cu_8Zr_3, Cu_2Zr, $Cu_{10}Zr_7$, $CuZr$, Cu_5Zr_7 and $CuZr_2$. Except the compound Cu_9Zr_2, they are treated as a line compound $(Al,Cu)_mZr_n$ with Al and Cu on the first sublattice and Zr on the second one in the Al–Cu–Zr system. The molar Gibbs energy of formula unit $(Al,Cu)_mZr_n$ is expressed as follows:

$$ G^{\phi}_m = y'_{\mathrm{Al}} G^{\phi}_{\mathrm{Al:Zr}} + y'_{\mathrm{Cu}} G^{\phi}_{\mathrm{Cu:Zr}} + mRT(y'_{\mathrm{Al}}\ \ln y'_{\mathrm{Al}} + y'_{\mathrm{Cu}}\ \ln y'_{\mathrm{Cu}}) + y'_{\mathrm{Al}} y'_{\mathrm{Cu}} \sum_j {}^{j}L^{\phi}_{\mathrm{Al,Cu:Zr}} (y'_{\mathrm{Al}} - y'_{\mathrm{Cu}})^j \tag{6} $$

where y'_{Al} and y'_{Cu} are the site fractions of Al and Cu on the first sublattice, respectively; $G^{\phi}_{\mathrm{Al:Zr}}$ and $G^{\phi}_{\mathrm{Cu:Zr}}$ are the molar Gibbs energy when the first sublattice is occupied by only one element Al or Cu, respectively; ${}^{j}L^{\phi}_{\mathrm{Al,Cu:Zr}}$ is the jth interaction parameter between elements Al and Cu on the first sublattice.

The compound Cu_9Zr_2 is described as $Cu_9(Al,Zr)_2$ with Cu on the first sublattice and Al and Zr on the second one. The molar Gibbs energy of the compound Cu_9Zr_2 is expressed as follows:

$$ G^{\mathrm{Cu_9Zr_2}}_m = y''_{\mathrm{Al}} G^{\mathrm{Cu_9Zr_2}}_{\mathrm{Cu:Al}} + y''_{\mathrm{Zr}} G^{\mathrm{Cu_9Zr_2}}_{\mathrm{Cu:Zr}} + 2RT(y''_{\mathrm{Al}}\ \ln y''_{\mathrm{Al}} + y''_{\mathrm{Zr}}\ \ln y''_{\mathrm{Zr}}) + y''_{\mathrm{Al}} y''_{\mathrm{Zr}} \sum_j {}^{j}L^{\mathrm{Cu_9Zr_2}}_{\mathrm{Cu:Al,Zr}} (y''_{\mathrm{Al}} - y''_{\mathrm{Zr}})^j \tag{7} $$

where y''_{Al} and y''_{Zr} are the site fractions of Al and Zr on the second sublattice, respectively; $G^{\mathrm{Cu_9Zr_2}}_{\mathrm{Cu:Al}}$ and $G^{\mathrm{Cu_9Zr_2}}_{\mathrm{Cu:Zr}}$ are the molar Gibbs energy when the second sublattice is occupied by only one element Al or Zr, respectively; ${}^{j}L^{\mathrm{Cu_9Zr_2}}_{\mathrm{Cu:Al,Zr}}$ is the jth interaction parameter between elements Al and Zr on the second sublattice.

The ternary compounds τ_1, τ_2, τ_4, τ_6, τ_9 and τ_{11} are described as a stoichiometric compound in the form of $Al_xCu_yZr_z$ in accordance with

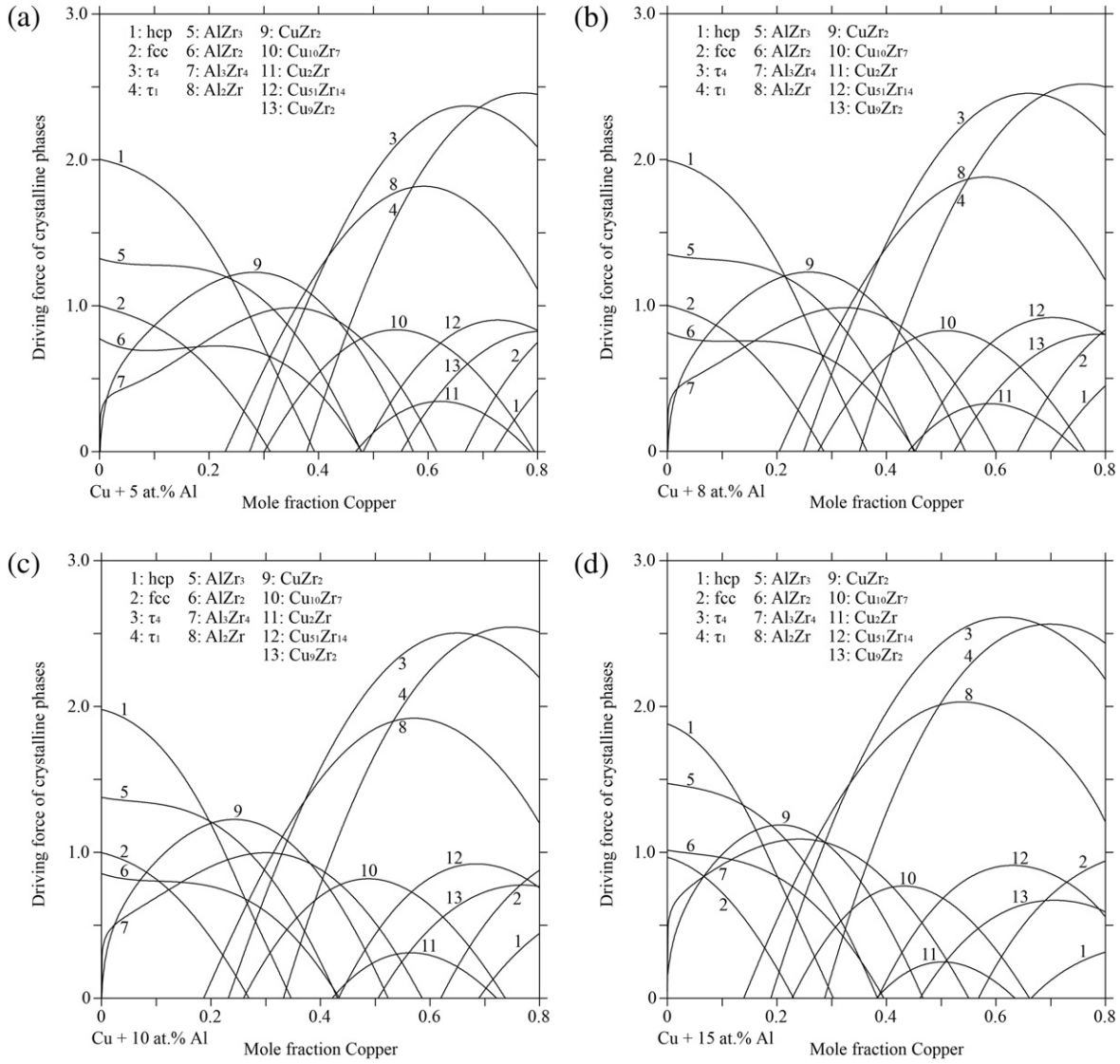

Fig. 14. a. Calculated driving force for crystalline phases from the supercooled liquids at 700 K and 5 at.% Al. b. Calculated driving force for crystalline phases from the supercooled liquids at 700 K and 8 at.% Al. c. Calculated driving force for crystalline phases from the supercooled liquids at 700 K and 10 at.% Al. d. Calculated driving force for crystalline phases from the supercooled liquids at 700 K and 15 at.% Al.

the experimental data [69]. The molar Gibbs energy of formula unit $Al_xCu_yZr_z$ is described as the following expression:

$$G_m^{Al_xCu_yZr_z} = x\mathrm{GHSER}_{Al} + y\mathrm{GHSER}_{Cu} + z\mathrm{GHSER}_{Zr} + c + dT \quad (8)$$

where c and d are the parameters to be optimized in the present work.

On the basis of the experimental information [69], the ternary compounds τ_3, τ_5, τ_7 and τ_8 are described as a line compound in the form of $(Al,Cu)_mZr_n$.

The ternary compounds τ_9' and τ_{10} are not considered in the present work in terms of the experimental data [64,70].

Thermodynamic models of the binary compounds in the Al–Zr and Cu–Zr systems and ternary compounds in the Al–Cu–Zr system relevant for this study are given in Table 1.

5. Assessment procedure

According to the published experimental information shown in Section 3, the Al–Cu–Zr system was assessed by means of the PARROT module of the thermodynamic software Thermo-Calc [73].

In the assessment procedure, the weight was chosen by the personal judgment and changed according to the error during the work until most of experimental phase equilibria and thermochemical data were reproduced well.

As a rule, the adjustable coefficients should be well selected according to the experimental data [74]. In order to make the model of the line compounds be close to the reality, a reasonable estimate should be made when the experimental data were not sufficient.

The thermodynamic parameters of the ternary liquid phase were obtained by combining the each binary parameters according to the experimental enthalpies of mixing of the liquid and undercooled liquid Al–Cu–Zr alloys [65]. Furthermore, the thermodynamic parameters of other phases were optimized on the basis of the following experimental information, including two invariant reactions in the Al-rich corner [64], the isothermal sections at 773 and 873 K in the Al-rich part [66], the isothermal sections at 1273 and 1373 K [69], and the isothermal section at 1073 K in the Zr-rich part [70].

6. Optimization results and discussions

The thermodynamic assessment of the Al–Cu–Zr system is performed in the present work and a set of self-consistent and reliable thermodynamic parameters is shown in Table 2.

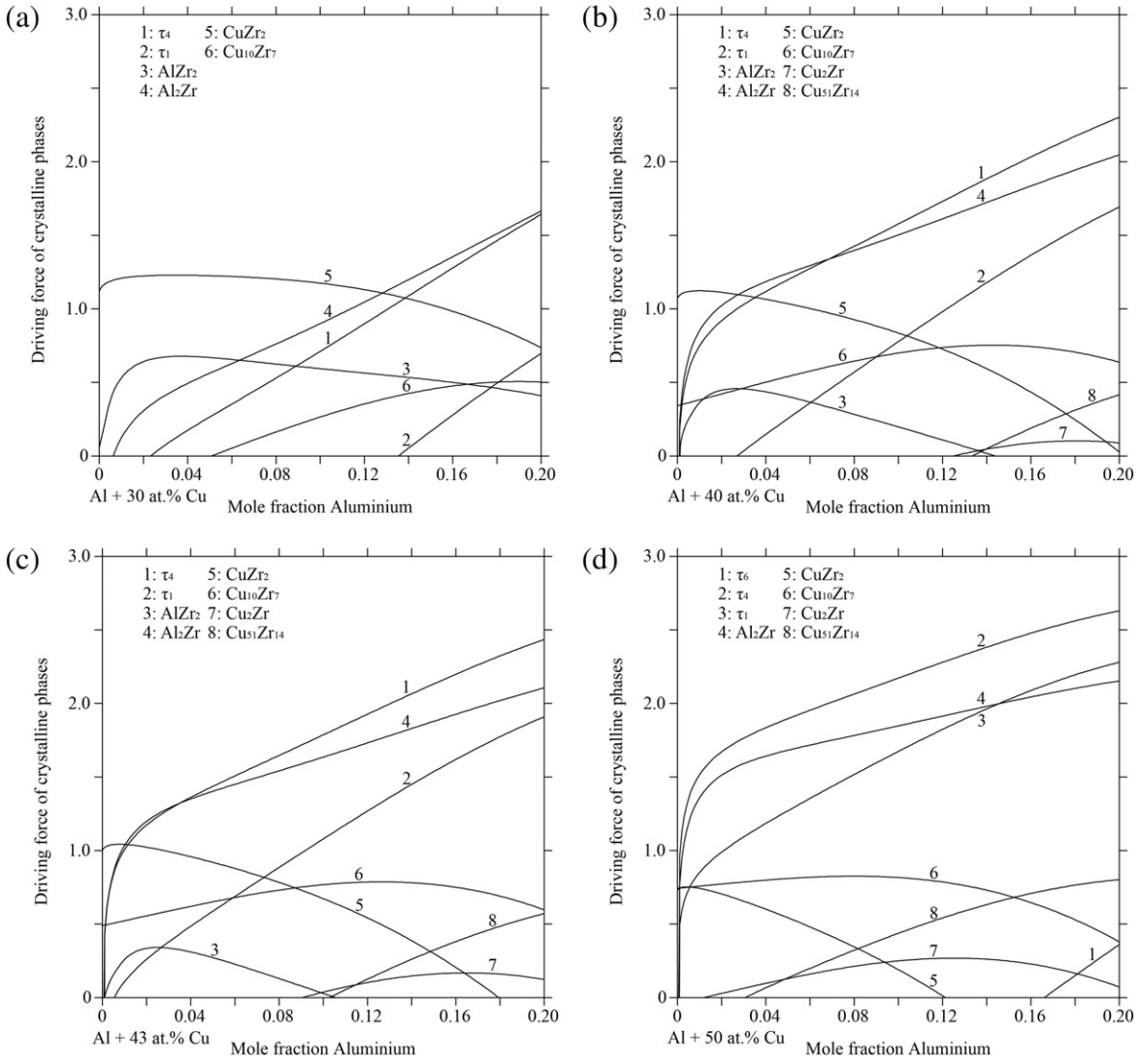

Fig. 15. a. Calculated driving force for crystalline phases from the supercooled liquids at 700 K and 30 at.% Cu. b. Calculated driving force for crystalline phases from the supercooled liquids at 700 K and 40 at.% Cu. c. Calculated driving force for crystalline phases from the supercooled liquids at 700 K and 43 at.% Cu. d. Calculated driving force for crystalline phases from the supercooled liquids at 700 K and 50 at.% Cu.

The calculated invariant reactions in the Al–Cu–Zr system are listed in Table 3. As shown in the table, a good agreement is obtained between the calculations and experiments [64]. The temperatures of the invariant reactions coincide exactly except the invariant reaction liq. + $\tau_8 \rightarrow \tau_7 + Al_3Zr$, in which the uncertainty is about 18 K, respectively. The reaction temperature of liq. + $\tau_8 \rightarrow \tau_7 + Al_3Zr$ could also been optimized to 1093 K [64]. However, the entropy of the zero-order interaction parameters of liquid phase almost needs +350 J/(K·mol of atoms), which is too large to be accepted in this work.

Figs. 4 and 5 present the calculated isothermal sections of the Al–Cu–Zr system at 1273 and 1373 K. The satisfied results are basically obtained, but some disagreements are still existed.

Two-phase regions related to the compounds, τ_5 and Al_4Zr_5 at 1373 K, and τ_5 and Al_3Zr_4 at 1273 K, are inconsistent with the experimental data [69]. From Ref. [69], the marked two-phase points as mentioned above are not located at the tie line connected by the corresponding phase boundary points. So these doubtful data are given less weight in the process of optimization, which may lead to somewhat different results.

Three-phase regions in the Cu-rich part related to the ternary compound τ_{11} are inconsistent with the experimental data [63], which is mainly resulted from the binary thermodynamic parameters of the liquid phase. In the process of optimization, the Gibbs energy of the ternary compound τ_{11} has been positive as much as possible on the assumption of ensuring the correctness of other phase relations.

The compound Al_4Zr_5 at 1273 K has a large solubilities in the present work but not of Wang et al. [69]. If the solubilities of the compound Al_4Zr_5 disappears at 1273 K, the total entropy of the interaction parameters almost needs + 120 J/(K·mol of atoms). So the entropy is set at the suitable value to ensure the rationality of the CALPHAD method in the present work.

Fig. 6 shows the calculated isothermal section of the Al–Cu–Zr system at 1073 K, which is in satisfactory agreement with the experimental data [70] except two-phase regions related to the compound $CuZr_2$ and τ_5. In the process of optimization, the complex models like τ_3 and simplified models like τ_4 are adopted based on their crystal structures and solubilities listed as Table 1, which will cause the composition deviation of the equilibrium points.

Table 4
Predicted alloy compositions of high glass-forming ability in the Al–Cu–Zr system.

Figure number	Compositions		
	x(Al)	x(Cu)	x(Zr)
14(a)	0.050	0.239	0.711
14(a)	0.050	0.378	0.572
14(a)	0.050	0.417	0.533
14(a)	0.050	0.694	0.256
14(b)	0.080	0.214	0.706
14(b)	0.080	0.350	0.570
14(b)	0.080	0.389	0.531
14(b)	0.080	0.688	0.232
14(c)	0.100	0.196	0.704
14(c)	0.100	0.204	0.696
14(c)	0.100	0.330	0.570
14(c)	0.100	0.369	0.531
14(c)	0.100	0.683	0.217
14(d)	0.150	0.139	0.711
14(d)	0.150	0.190	0.660
14(d)	0.150	0.274	0.576
14(d)	0.150	0.333	0.517
14(d)	0.150	0.682	0.168
15(a)	0.128	0.300	0.572
15(b)	0.028	0.400	0.572
15(b)	0.067	0.400	0.533
15(c)	0.010	0.430	0.560
15(c)	0.033	0.430	0.537
15(d)	0.001	0.500	0.499

Figs. 7 and 8 show the calculated isothermal sections of the Al–Cu–Zr system at 773 and 873 K, which fit well to the results reviewed by Tretyachenko [66].

Figs. 9 and 10 are the calculated vertical sections of the Al–Cu–Zr system at a constant composition of 20 at.% Al and ratio of Cu:Zr = 1:1, which shows that the optimized thermodynamic parameters in this work are appropriate.

Fig. 11 shows the calculated enthalpies of mixing of ternary liquid and undercooled liquid Al–Cu–Zr alloys, and the results are in satisfactory agreement with the experimental measurements [65]. Some deviation still exists in Fig. 11 a and c, which is mainly due to the difference for the binary enthalpies of mixing between the optimized results [36,49,57] and the experimental data [65,75,76].

Fig. 12 is the calculated projection of the liquidus surface in the Al–Cu–Zr system.

Fig. 13 is the calculated reaction scheme in the Al–Cu–Zr system.

7. Prediction of glass-forming ability

Boettinger [26] proposes that the formation process of glass is described as a competition between the crystalline phases and supercooled liquids, and the low crystal growth ability should promote the formation of BMGs. With the help of the method, GFA is estimated by searching the local minimum of the driving force for crystalline phase from the supercooled liquids.

The GFA of many Al–Cu–Zr alloys have been investigated by several researchers [2–4], which show that the glass transition temperatures at different compositions are within a range from 670 to 730 K. Therefore in the present work, the temperature at 700 K is selected for prediction of high GFA.

Figs. 14 and 15 show the calculated driving force for crystalline phase from the supercooled liquids at 700 K and eight groups of compositions. The calculated data points with the local minimum of the driving force have been sorted out and further summarized on Table 4.

Fig. 16 presents the predicted alloy compositions of high GFA by searching the local minimum of the driving force compared with the experimental data [2–4]. The filled black triangles represent the calculated alloy compositions from Table 4. In general, the eutectic compositions relate to high GFA due to the minimum liquidus temperature. Compared with the eutectic compositions in Fig. 12, the alloys with high GFA in the Al–Cu–Zr system by experiment or calculation are off-eutectic. In other words, high GFA prediction with the help of eutectic points is not enough in the Al–Cu–Zr system. The predicted alloy compositions of high GFA by searching the local minimum of the driving force in the Al–Cu–Zr system reproduces the experimental measurements well on the whole. It is clear that the driving force criterion has its advantages and can be used as an index to predict alloy compositions of high GFA in the multicomponent system.

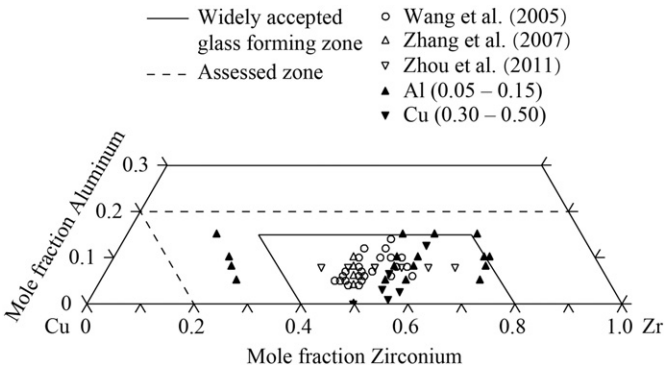

Fig. 16. Predicted alloy compositions of high glass-forming ability by searching the local minimum driving force for crystalline phases compared with the experimental data [2–4].

8. Conclusion

In terms of the available experimental information, a set of self-consistent and reliable thermodynamic parameters of the Al–Cu–Zr system is obtained. The calculated enthalpies of mixing of the liquid phase, invariant reactions, and isothermal sections of the Al–Cu–Zr system show a good consistency with the experimental data. With the optimized thermodynamic parameters, a variety of thermodynamic calculations of practical interest can be made.

The calculated projection of the liquidus surface and reaction scheme in the Al–Cu–Zr system can be used as building blocks for further experimental studies. The predicted alloy compositions of high GFA show good agreement with the experimental results and can provide a guidance for further alloy design of Al–Cu–Zr BMGs.

Acknowledgement

This work was supported by National Natural Science Foundation of China (NSFC) (grant nos. 51371029 and 51671025) and the National Key Research and Development Program (grant no. 2016YFB0701401).

Appendix A. Supplementary data

Supplementary data to this article can be found online at http://dx.doi.org/10.1016/j.jnoncrysol.2016.09.031.

References

[1] A. Inoue, Acta Mater. 48 (2000) 279–306.
[2] D. Wang, H. Tan, Y. Li, Acta Mater. 53 (2005) 2969–2979.
[3] Q. Zhang, W. Zhang, G. Xie, A. Inoue, Mater. Trans. 48 (2007) 1626–1630.
[4] B.W. Zhou, X.G. Zhang, W. Zhang, H. Kimura, A. Makino, A. Inoue, Mater. Res. Innov. 15 (2011) 310–313.
[5] Q.K. Jiang, X.P. Nie, Y.G. Li, Y. Jin, Z.Y. Chang, X.M. Huang, J.Z. Jiang, J. Alloys Compd. 443 (2007) 191–194.
[6] H.F. Li, Y.F. Zheng, F. Xu, J.Z. Jiang, Mater. Lett. 75 (2012) 74–76.
[7] S. Buzzi, K. Jin, P.J. Uggowitzer, S. Tosatti, I. Gerber, J.F. Löffler, Intermetallics 14 (2006) 729–734.
[8] Q.S. Zhang, W. Zhang, A. Inoue, Scr. Mater. 61 (2009) 241–244.
[9] Y.-S. Sun, W. Zhang, W. Kai, P.K. Liaw, H.-H. Huang, J. Alloys Compd. 586 (2014) S539–S543.
[10] Q. He, Y.-Q. Cheng, E. Ma, J. Xu, Acta Mater. 59 (2011) 202–215.
[11] Q. He, J.K. Shang, E. Ma, J. Xu, Acta Mater. 60 (2012) 4940–4949.
[12] E.S. Park, D.H. Kim, Acta Mater. 54 (2006) 2597–2604.
[13] J. Chen, Y. Zhang, J.P. He, K.F. Yao, B.C. Wei, G.L. Chen, Scr. Mater. 54 (2006) 1351–1355.
[14] K. Zhou, Y. Liu, S. Pang, T. Zhang, J. Alloys Compd. 656 (2016) 389–394.
[15] L. Liu, C.L. Qiu, C.Y. Huang, Y. Yu, H. Huang, S.M. Zhang, Intermetallics 17 (2009) 235–240.
[16] L. Huang, Y. Yokoyama, W. Wu, P.K. Liaw, S. Pang, A. Inoue, T. Zhang, W. He, J. Biomed, Mater. Res. Part B 100B (2012) 1472–1482.
[17] S. Zhu, G. Xie, F. Qin, X. Wang, A. Inoue, J. Mech. Behav. Biomed. Mater. 13 (2012) 166–173.
[18] A.L. Greer, Nature 366 (1993) 303–304.
[19] H.S. Chen, Acta Metall. 22 (1974) 1505–1511.
[20] H.S. Chen, Rep. Prog. Phys. 43 (1980) 353–432.
[21] Z.P. Lu, C.T. Liu, Acta Mater. 50 (2002) 3501–3512.
[22] Q. Chen, J. Shen, D. Zhang, H. Fan, J. Sun, D.G. McCartney, Mater. Sci. Eng. A 433 (2006) 155–160.
[23] R. Bormann, Mater. Sci. Eng. A 178 (1994) 55–60.
[24] J. Ågren, B. Cheynet, M.T. Clavaguera-Mora, K. Hack, J. Hertz, F. Sommer, U. Kattner, Calphad 19 (1995) 449–480.
[25] G. Shao, B. Lu, Y.Q. Liu, P. Tsakiropoulos, Intermetallics 13 (2005) 409–414.
[26] W.J. Boettinger, Growth kinetic limitations during rapid solidification, in: B.H. Kear, B.C. Giessen, M. Cohen (Eds.), Rapidly Solidified Amorphous and Crystalline Alloys, Elsevier, Amsterdam 1982, p. 15.
[27] D. Kim, B.-J. Lee, N.J. Kim, Intermetallics 12 (2004) 1103–1107.
[28] D. Kim, B.-J. Lee, N.J. Kim, Scr. Mater. 52 (2005) 969–972.
[29] S. Gorsse, G. Orveillon, O.N. Senkov, D.B. Miracle, Phys. Rev. B 73 (2006) 224201-1–224202-9.
[30] L.G. Zhang, H.Q. Dong, J.F. Nie, F.G. Meng, S. Jin, L.B. Liu, Z.P. Jin, J. Alloys Compd. 491 (2010) 123–130.
[31] C. Li, S. Chen, Z. Du, C. Guo, N. Wang, Intermetallics 19 (2011) 1678–1682.
[32] N. Saunders, Al–Cu system, in: I. Ansara, A.T. Dinsdale, M.H. Rand (Eds.), COST 507 Thermochemical Database for Light Metal Alloys, 2, European Commission 1998, pp. 28–33.
[33] H. Liang, Y.A. Chang, J. Phase Equilib. 19 (1998) 25–37.
[34] J. Miettinen, Calphad 26 (2002) 119–139.
[35] V.T. Witusiewicz, U. Hecht, S.G. Fries, S. Rex, J. Alloys Compd. 385 (2004) 133–143.
[36] S.-M. Liang, R. Schmid-Fetzer, Calphad 51 (2015) 252–260.
[37] N. Saunders, V.G. Rivlin, Mater. Sci. Technol. 2 (1986) 521–527.
[38] N. Saunders, Z. Metallkd. 80 (1989) 894–903.
[39] S.V. Meschel, O.J. Kleppa, J. Alloys Compd. 191 (1993) 111–116.
[40] P. Klein, I. Jacob, P.A.G. O'Hare, R.N. Goldberg, J. Chem. Thermodyn. 26 (1994) 599–608.
[41] A. Peruzzi, J. Nucl. Mater. 186 (1992) 89–99.
[42] T. Wang, Z.P. Jin, J.-C. Zhao, J. Phase Equilib. 22 (2001) 544–551.
[43] G. Ghosh, M. Asta, Acta Mater. 53 (2005) 3225–3252.
[44] H. Zhang, S. Wang, J. Mater. Res. 25 (2010) 1689–1694.
[45] M. Mihalkovic, M. Widom, et al., Alloy Database, http://www.alloy.phys.cmu.edu.
[46] C. Colinet, J.-C. Crivello, J.-C. Tedenac, J. Solid State Chem. 205 (2013) 217–224.
[47] J.E. Saal, S. Kirklin, M. Aykol, B. Meredig, C. Wolverton, J. Min. Met. Mater. Soc. 65 (2013) 1501–1509.
[48] Y.H. Duan, B. Huang, Y. Sun, M.J. Peng, S.G. Zhou, J. Alloys Compd. 590 (2014) 50–60.
[49] E. Fischer, C. Colinet, J. Phase Equilib. 36 (2015) 404–413.
[50] N. Saunders, Calphad 9 (1985) 297–309.
[51] K.-J. Zeng, M. Hämäläinen, J. Phase Equilib. 15 (1994) 577–586.
[52] X.C. He, H. Wang, H.S. Liu, Z.P. Lin, Calphad 30 (2006) 367–374.
[53] T. Abe, M. Shimono, M. Ode, H. Onodera, Acta Mater. 54 (2006) 909–915.
[54] N. Wang, C. Li, Z. Du, F. Wang, W. Zhang, Calphad 30 (2006) 461–469.
[55] K. Yamaguchi, Y.-C. Song, T. Yoshida, K. Itagaki, J. Alloys Compd. 452 (2008) 73–79.
[56] D.H. Kang, I.-H. Jung, Intermetallics 18 (2010) 815–833.
[57] W. Gierlotka, K.-C. Zhang, Y.-P. Chang, J. Alloys Compd. 509 (2011) 8313–8318.
[58] O.S. Zarechnyuk, A.N. Malinkovich, E.A. Lalayan, Izv. Akad. Nauk. SSSR Met. 6 (1967) 201–204.
[59] V.Y. Markiv, V.V. Burnashova, Poroshk. Metall. 12 (1970) 53–58.
[60] R.M.z. Reckendorf, P.C. Schmidt, A. Weiss, Z. Physik, Chemie Neue Folge 163 (1989) 103–108.
[61] R.M.z. Reckendorf, P.C. Schmidt, A. Weiss, J. Less-Common Met. 159 (1990) 277–289.
[62] R.M.z. Reckendorf, P.C. Schmidt, A. Weiss, J. Less-Common Met. 159 (1990) 291–298.
[63] L.A. Tretyachenko, in: G. Effenberg (Ed.), Al–Cu–Zr Ternary Phase Diagram Evaluation, MSI Eureka, Materials Science International Services GmbH, Stuttgart, 1992.
[64] D. Soares, F. Castro, J. Chim. Phys. 94 (1997) 958–963.
[65] V. Witusiewicz, U.K. Stolz, I. Arpshofen, F. Sommer, Z. Metallkd. 89 (1998) 704–713.
[66] L.A. Tretyachenko, Al–Cu–Zr (aluminium–copper–zirconium), in: G. Effenberg, S. Llyenko (Eds.), Landolt-Börnstein-Group IV Physical Chemistry, vol.11 A2, Light Metal Systems, Part2, Springer-Verlag, Germany 2005, pp. 206–222.
[67] H. Bo, J. Wang, S. Jin, H.Y. Qi, X.L. Yuan, L.B. Liu, Z.P. Jin, Intermetallics 18 (2010) 2322–2327.
[68] V. Raghavan, J. Phase Equilib. 32 (2011) 452–454.
[69] C.P. Wang, S.B. Tu, Y. Yu, J.J. Han, X.J. Liu, Intermetallics 31 (2012) 1–8.
[70] K.B. Kalmykov, N.E. Dmitrieva, N.L. Zvereva, S.F. Dunaev, D.M. Komdrat'ev, Mosc. Univ. Chem. Bull. 67 (2012) 171–176.
[71] A.T. Dinsdale, Calphad 15 (1991) 317–425.
[72] O. Redlich, A.T. Kister, Ind. Eng. Chem. 40 (1948) 345–348.
[73] Thermo-Calc Software AB, http://www.thermocalc.com.
[74] H.L. Lukas, S.G. Fries, J. Phase Equilib. 13 (1992) 532–542.
[75] U.K. Stolz, I. Arpshofen, F. Sommer, B. Predel, J. Phase Equilib. 14 (1993) 473–478.
[76] V. Witusiewicz, I. Arpshofen, F. Sommer, Z. Metallkd. 88 (1997) 866–872.